

Data and Methods for Estimating the Severity of Minor Impacts

Mark N. Bailey, Bing C. Wong, and Jonathan M. Lawrence
MacInnis Engineering Associates Ltd.

ABSTRACT

Front, rear, lateral and side-swipe collisions were staged to correlate passenger vehicle damage to motion. Data from the staged collisions are used to develop severity-prediction methods for the four collision types. Human volunteers were present in many of the vehicles tested. Their responses, and the responses of human volunteers to staged impacts in other studies, are discussed in terms of impact severity.

For front and rear impacts, data are presented that correlate the post-impact condition of bumper systems to impact severity. These data build on data previously presented^{1,2,3}. A method for computing velocity change (ΔV) for vehicle to vehicle collisions from vehicle to barrier data is presented.

Data from staged low-speed lateral collisions correlate target and bullet vehicle damage to linear and angular velocity change (ΔV , $\Delta \omega$), impact location, pavement friction and collision force. It is shown how momentum, energy and restitution principles can be used to predict ΔV and $\Delta \omega$ from damage.

For staged side-swipe collisions, damage details are correlated to the target vehicle acceleration-time history. The vehicle motion is characterized as a vibration dose.

INTRODUCTION

Four types of "minor" collisions frequently occur. These are rear-end, front-end, lateral, and side-swipe, (Figure 1). Our previous work has concentrated on bumper properties and their relevance to "minor" rear-end impacts¹⁻³. The term "minor" is used to describe impacts where tire forces and/or restitution effects cannot be ignored. It is not used to reference vehicle damage or occupant symptoms.

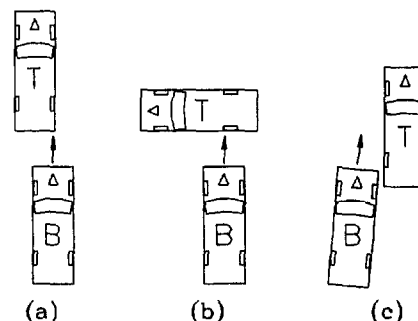


Figure 1. (a) rear and front-end; (b) lateral; (c) side-swipe
For any of the four types of collisions, the usual question put to investigators is:

Are individuals who have experienced an apparently minor collision at risk of injury?

The diagnosis of injuries arising out of a minor collision is usually subjective. Objective clinical findings are often absent. The mechanism of a possible injury is not always well understood, so may sometimes be dismissed as being altogether absent. For example, it is unclear how neck or back symptoms occur in low-speed rear-end collisions when there is good head support. It may be, based on human volunteer tests (see McConnell et al⁴), that one possible injury mechanism is a rapid compression-tension cycle applied to the neck rather than, or in addition to, neck hyperextension. If that is the case, a neck injury mechanism can operate despite the head restraint. The type of detailed investigation that lead to that finding must

- 1) guide researchers to establish reasonable levels where symptoms can be produced,
- 2) identify injury mechanisms, and
- 3) devise safety measures to interrupt these mechanisms.

Data and methods in this paper focus on (1) above by relating levels of impact to the presence or absence of occupant symptoms. Vehicle motion, and meaningful ways to quantify it, are examined in four

types of minor collisions. The following descriptors of impact severity are discussed:

rear-end, front-end	ΔV
lateral	ΔV or $\Delta \omega$
side-swipe	$a(t)$, or $[a^4(t)dt]^{0.25}$

For staged collisions with human volunteers, impact severity is compared to the post-collision volunteer condition. Seat, posture, preparedness and physical condition are not included in the comparison. The volunteers were not instrumented, and only general details of their motion are discussed.

BACKGROUND

In collisions where a vehicle has permanent damage, for example several centimeters of frontal crush from an intersection collision, the amount of damage can be correlated to the collision severity. The method was first introduced by Campbell⁵, and has been adopted by various computer programs. An investigator attempts to quantify severity in terms of ΔV , the abrupt change in velocity of the vehicle's centre of mass from collision with another vehicle. ΔV follows directly from the crush of both vehicles. The correlation between crush and ΔV is made from a linear force-crush model, with two empirical coefficients determined from crash testing, then applying that to determine energy absorption, and finally ΔV .

Mathematically, from conservation of energy and conservation of momentum, it can be shown that for a plastic collision

$$\Delta V_1 = \sqrt{\frac{2(E_1 + E_2)(m_1 + m_2)}{m_1 m_2}} \quad (1)$$

where ΔV_1 is the velocity change of one vehicle, E_1 and E_2 is the energy absorbed by each vehicle (related to amount of damage), and m_1 and m_2 are the vehicle masses. The energy absorbed is determined from the degree of crush. In the absence of a direct correlation between energy absorption and crush, the energy absorbed is determined as follows (for the special case of uniform crush):

$$E_1 = L \left[AC + \frac{BC^2}{2} + \frac{A^2}{2B} \right] \quad (2)$$

where L is the crush width and C is the uniform crush depth. E_2 may be found similarly. The constants A and B are vehicle specific, and are different for the front, back and sides. Central to the method is the force-crush relationship, which incorporates the A and B coefficients.

$$F = A + Bx \quad (3)$$

where F is the force per unit width and x is the average crush depth. This model, while inappropriate for minor impacts, is used for higher speed impacts where there is plastic deformation. The complete energy absorption versus crush relation for a vehicle (an alternative to the force-crush model) would yield better results, though the economics are prohibitive. It should be noted that the ΔV is considered "brief", on the order of 100 to 200 ms. It is implicit that any differences between duration in a barrier collision and a vehicle-to-vehicle collision do not affect the force-crush model because the structures are not strain rate sensitive at the speeds under consideration.

An important assumption of the method is that restitution effects and tire forces are small enough to be neglected. However, at lower speeds restitution is significant, and the collision force is often not small compared to available tire traction.

Another measure of severity, similar to ΔV , is the EBS (equivalent barrier speed), also referred to as the BEV (barrier equivalent velocity). Setting E_2 to zero and m_2 to infinity in Equation 1 yields the EBS. The EBS will be equal in magnitude to ΔV only in certain cases. The reader is referred to articles by Hight⁶ and Varat⁷ for further explanation. Specifically, in a plastic impact the ΔV and the EBS will be equal when the vehicle stiffnesses and masses are equal.

In attempting to estimate ΔV in minor rear-end, front-end and lateral collisions, methods analogous to the foregoing have been developed, with these additional factors included in the analysis:

- restitution is accounted for
- tire forces are accounted for
- direct energy-deformation data are used, so that a force-deformation model is unnecessary

Restitution is accounted for by including the equation for restitution with the momentum and energy equations. Tire impulse forces are accounted for with an $F\Delta t$ term in the momentum equation. A large quantity of energy-deformation data have been gathered for many vehicles in non-plastic impacts (in low-speed front or rear impacts the damage is slight or nil and the same vehicle can be tested repeatedly; several energy absorption-deformation data points can be acquired for the same vehicle). For a minor collision, it is a matter of correlating the damage with the energy absorbed, then solving the appropriate momentum, energy and restitution equations to estimate the ΔV .

An alternative method is to scale the EBS of one vehicle by a factor relating mass and stiffness of both vehicles,

$$\Delta V_1 = EBS_1 \sqrt{(m_2/(m_1 + m_2))((k_1 + k_2)/k_2)}$$

which is only applicable for higher speed impacts. That method can make use of the force-crush model discussed above, which implies energy absorption is of the form $E = \frac{1}{2}kd^2$, where k is stiffness (force per unit crush) and d is deformation or crush. If energy versus deformation is quadratic in a bumper impact, results identical to the direct energy method can be anticipated if restitution is accounted for and tire effects are ignored.

EXPERIMENTAL PROCEDURE

All the vehicles that were tested met Canadian Motor Vehicle Safety Standards (CMVSS). As such, all vehicles had bumpers that met CMVSS 215, which stipulates that passenger cars must be free of lamp, lens and fuel tank damage and must be driveable after 8 km/h front and rear barrier impacts and 5 km/h corner impacts and 8 km/h pendulum impacts. The post-impact condition of the bumpers is exempted in the standard.

Front and rear collision data have been recorded for vehicle-to-vehicle and vehicle-to-barrier tests. For vehicle-to-vehicle tests the bullet vehicle was either driven or pushed into the stationary target vehicle. In all tests with volunteers the bullet vehicle was pushed and its engine was off. The vehicles had MEA 5th wheels attached to their sides which recorded vehicle position at 128 or 200 Hz. Some vehicles also had strain-gage type accelerometers mounted laterally and/or longitudinally on the transmission tunnel. From the 5th wheel data, time-varying velocity and acceleration can be derived. Figure 2 shows a 5th wheel velocity trace for a vehicle-to-barrier collision. Figure 3 shows acceleration derived from the same data shown in Figure 2. Acceleration from the 5th wheel is derived from a quadratic least squares moving average⁸. The acceleration compares favorably with the acceleration measured directly with an accelerometer mounted on the vehicle's transmission tunnel and from two load cells in the barrier at the bumper level.

Target/bullet vehicle pairs were usually collided several times at increasing severity and details of bumper or other damage were recorded after each individual collision. When volunteer occupants were present in the target vehicle the rear view mirrors were covered or removed so that there was no visual stimulus for the volunteer occupant to respond to. With the engine of the bullet vehicle off, there was also no audible stimulus for the volunteer. The volunteer occupants in all rear-end tests were asked to relax, but knew that an impact would occur in a

matter of minutes. Occupants in all front-end tests did not have any stimuli masked. Volunteers were asked to report any symptoms immediately after each test, and in the days following the test. For vehicle-to-barrier tests the vehicles were pushed frontwards or backwards into a rigid barrier. The barrier consists of two steel floor mounted trusses with a horizontal steel beam. The beam can be raised or lowered to accommodate varying bumper heights. A 10,000 lb (44,500 N) load cell is fitted between the horizontal beam and each vertical truss (two load cells total). Vehicles that were pushed into the barrier were fitted with an MEA 5th wheel mounted to the side. Biaxial accelerometers were also mounted to the transmission tunnels of some vehicles. Data were recorded at 128 or 200 Hz. As in the vehicle-to-vehicle tests, visual and audio stimuli were removed as much as possible for the collisions with volunteer occupants. However, a volunteer facing forward in a backward moving vehicle knows when the impact will occur due to his/her view of the surroundings and initial separation from the barrier. Initial separation from the barrier was about 10m or less for most tests.

Lateral collisions were staged on a level concrete or asphalt surface. The angle between adjacent sides of the vehicles was 90°. The bullet vehicle was equipped in each case with a 5th wheel mounted to its left or right side. In Tests 1 through 4 there were MEA 5th wheels mounted to the target and bullet vehicles to measure their forward velocities. The target 5th wheel had a pivoted rear mount to prevent damage from lateral post-impact movement. Two accelerometers were mounted on the transmission tunnel of the Toyota to measure lateral and longitudinal acceleration.

In tests 18 to 21 the bullet vehicle had two 10000 lb (44500 N) load cells mounted between its bumper beam and its bumper isolators, and an MEA 5th wheel was mounted on the target vehicle rear bumper parallel to the bumper to measure angular speed. Two uni-axial accelerometers were mounted on the target vehicle, one on the transmission tunnel and one directly above on top of the roof. The sensitive axes were oriented transverse to the vehicle's longitudinal axis to record lateral acceleration. The target vehicles were weighed to determine their overall and individual axle weights.

Side-swipe collisions 22 to 24 used the same bullet/target vehicle pair used in lateral tests 18 to 21. The lateral collisions were done on the vehicle right (passenger) side and the side-swipe tests were done on the left (driver's) side. The same instrumentation was used as in the lateral tests, except that the 5th wheel on the target vehicle was swung around parallel to the vehicle longitudinal axis and the roof. For side-swipe tests SS8 to SS19, the bullet vehicle was

equipped with a MEA 5th wheel and the target vehicle had accelerometers mounted at the vehicle centreline ahead of the front seats to measure longitudinal and lateral acceleration at 200 Hz.

Procedures similar to those used in the rear-end tests were used for target vehicle volunteers in the side-swipe tests. For lateral tests, the procedure was similar to the front-end tests.

In most of the front-end and rear-end collisions there was no vehicle damage. In the lateral and side-swipe collisions there was body panel damage to the target vehicle in all but the most trivial tests. In some of those tests, the same portion of the vehicle body was struck more than once. Attempts were made to discriminate the damage from each test, even though a single body panel may have had damage from multiple impacts.

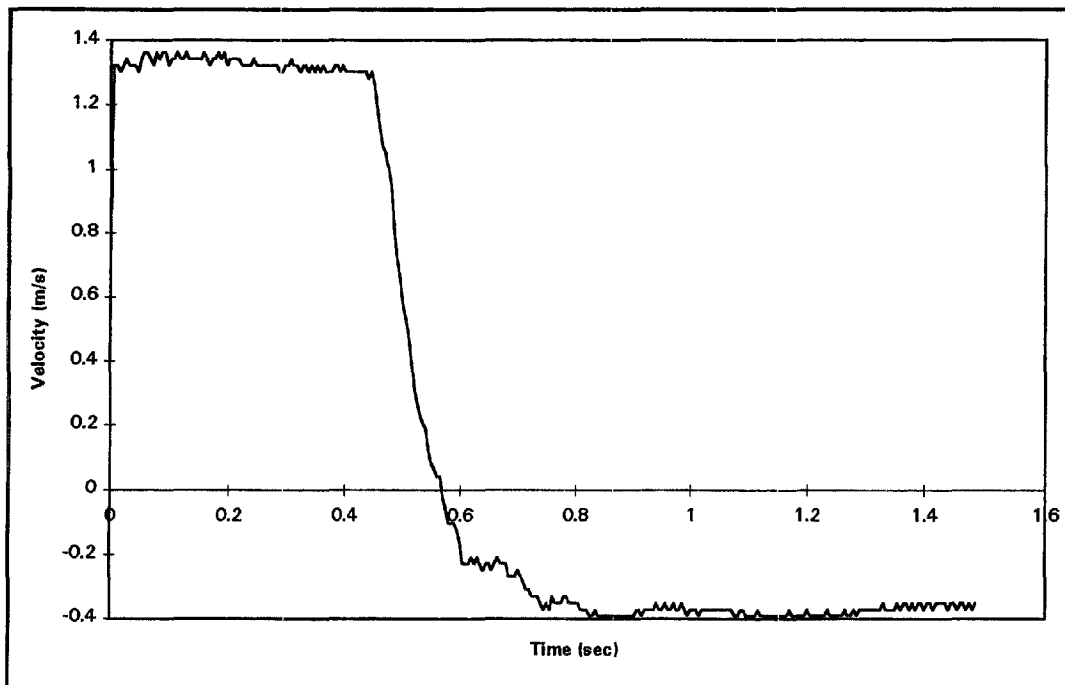


Figure 2. 5th Wheel trace, vehicle-to-barrier collision. The speed drops below zero when the vehicle rebounds backwards from the barrier.

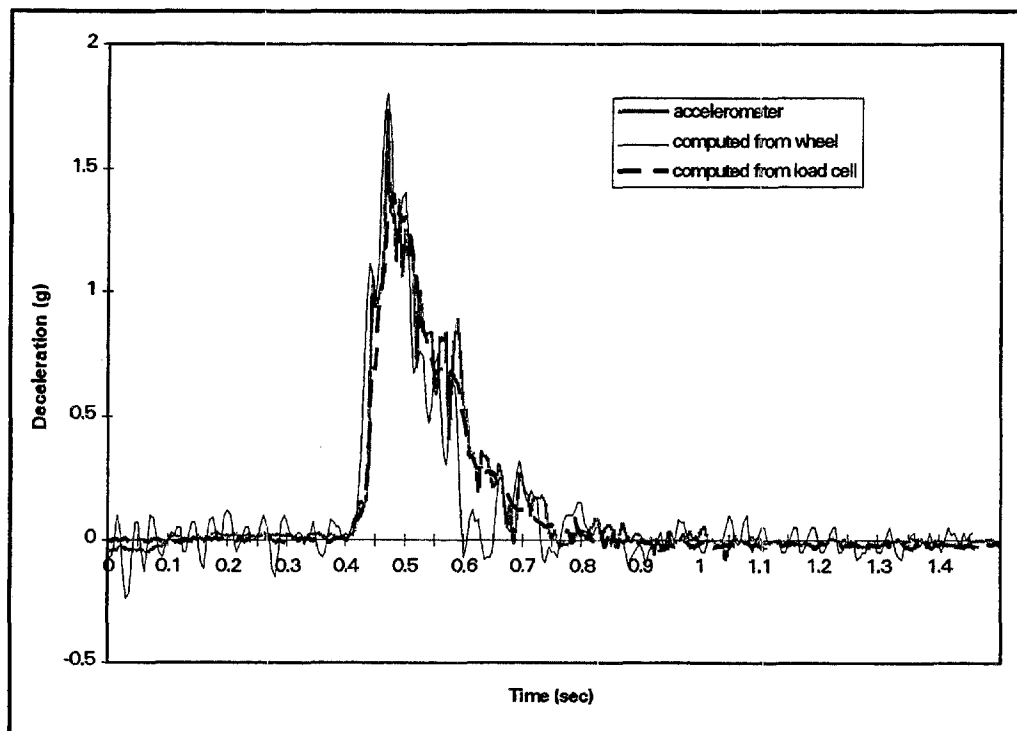


Figure 3. Comparison of vehicle acceleration from three sources: 5th wheel, accelerometer and load cells.

REAR-END AND FRONT-END COLLISIONS

For characterizing severity in rear or front impacts it is useful to use the concept of *velocity change* or *delta V* (ΔV). ΔV is defined as the change in a vehicle's speed and direction that takes place over the brief duration of an impact. Hence impact severity is often quantified as 'km/h ΔV '.

A vehicle's velocity change can be positive or negative. For the vehicle struck from behind, the "target" vehicle, the velocity change is positive: its speed an instant after the impact is greater than it was before the impact. For the striking, or "bullet", vehicle the velocity change is negative, because its speed an instant after the impact is lower than it was before the impact. The terms velocity change and speed change are often used interchangeably.

Figure 4 shows schematically the concept of velocity change in a low speed rear impact. The stationary front car (the target) is hit by the rear car moving at 10 km/h (the bullet). After the vehicles collide and separate, the target has a velocity of 7 km/h. Since its initial velocity was zero, its velocity change was 7 km/h (impact severity = 7 km/h ΔV).

Figure 5 shows the related concept of Equivalent Barrier Speed (EBS). The car (same as the target in Figure 3) moves backward toward the barrier at 5 km/h. It hits the barrier and rebounds forward at

2 km/h, a velocity change of 7 km/h (impact severity = 7 km/h ΔV). It hit the barrier at 5 km/h, which is, by definition, its EBS.

For the same impact speed, different cars will rebound at different speeds (because of different restitution). A different rebound speed results in a different velocity change for the same EBS.

In many cases the amount of compression of a bumper component can be correlated to the vehicle's velocity change or EBS in a minor front or rear impact (see References 1-3). For example, many vehicles are equipped with bumper isolators. An isolator is a piston and cylinder assembly that attaches the bumper to the car. A pair of isolators, but sometimes three, are attached at one end to the car and at the other end to a metal or plastic bumper beam. The isolators are parallel to the vehicle longitudinal axis. The isolator is filled with compressed gas (to act as a spring) and oil (to absorb energy when forced through and orifice) or a silicone gel. Often, when an isolator has been compressed there will be an observable scrape mark on the piston showing how far it compressed. The amount of compression can lead to conclusions about the severity of the impact. Isolators are found on many North American cars. For a complete description of isolators, see References 2 and 3 and the standard SAE J1571.

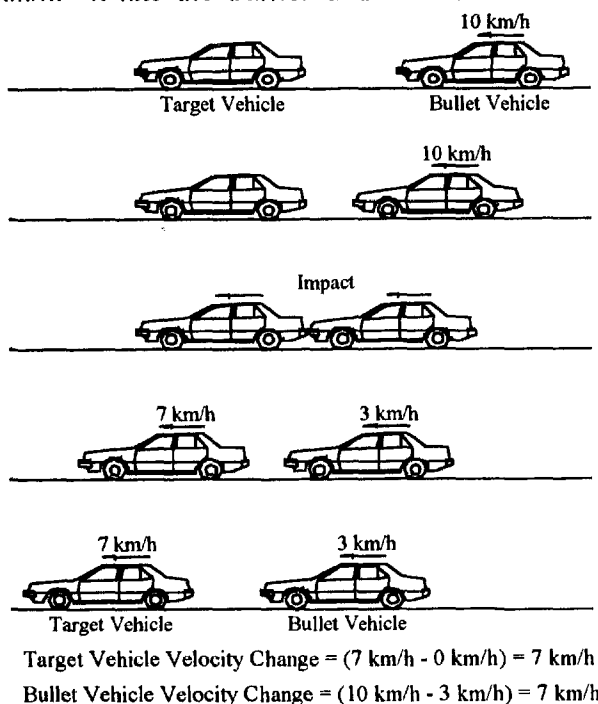


Figure 4. Velocity change.

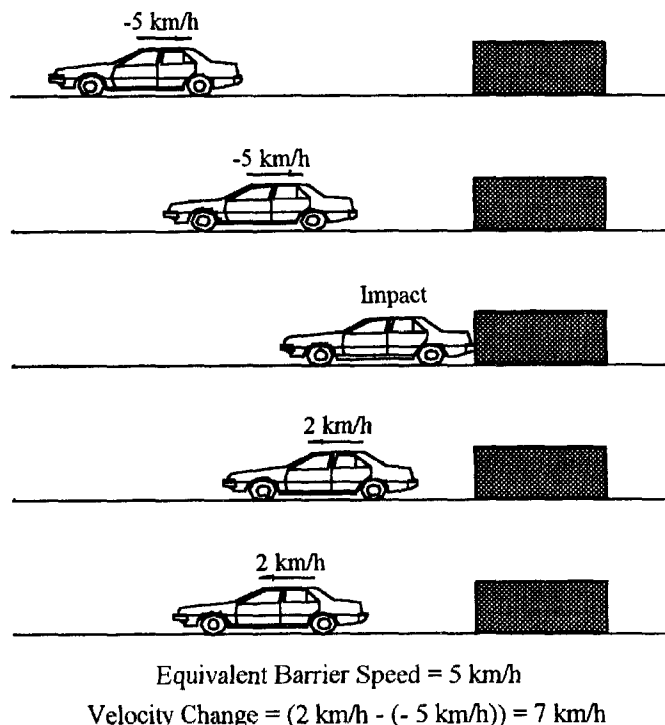


Figure 5. Equivalent barrier speed.

SEVERITY PREDICTION (FRONT, REAR-END)

It is desirable to be able to predict ΔV in a vehicle-to-vehicle impact from vehicle-to-barrier test data, as in higher speed collisions. MacInnis Engineering has staged over one thousand vehicle-to-barrier collisions, so the properties of many specific vehicles are known. These data can be applied to vehicle-to-vehicle collisions either directly, or using a momentum-energy-restitution model.

The correlation between ΔV and isolator compression is approximately the same for vehicle-to-vehicle and vehicle-to-barrier collisions, provided the mass ratio of the vehicles is not too different from unity, and provided the bumper isolators on each vehicle have similar stiffnesses.

When the mass ratio is much different from unity, or when the isolators have different stiffnesses, direct application of the vehicle-to-barrier data to determining the ΔV for a vehicle-to-vehicle collision may lead to an over or underestimate. This is demonstrated by a series of impacts involving a 1982 Ford Granada (bullet) and a 1976 Volkswagen Rabbit (target). The bullet:target mass ratio was 1.73:1. Vehicle-to-barrier data were gathered for the rear of the Volkswagen and the front of the Granada. Subsequently, the same two vehicles were involved in four vehicle-to-vehicle collisions. Isolator compression and pre-and post impact speeds were recorded for each vehicle for each impact. Figure 6 shows 5th wheel data for a vehicle-to-vehicle impact between the back of the Volkswagen and the front of the Ford. The 1282 kg Ford has a smaller ΔV than the 740 kg Volkswagen.

From these data, vehicle-to-vehicle and vehicle-to-barrier data were compared for the Volkswagen. Figure 7 shows that direct application of the vehicle-to-barrier data to these vehicle-to-vehicle impacts would overestimate the Volkswagen ΔV .

The more complex momentum-energy-restitution method, presented previously¹, can be used to predict the severity of the vehicle-to-vehicle impacts from vehicle-to-barrier data. The equations are as follows:

Conservation of Momentum

$$M_t V_t + M_b V_b = M_t V'_t + M_b V'_b + F \Delta t \quad (4)$$

Conservation of Energy.

$$\frac{1}{2} M_t V_t^2 + \frac{1}{2} M_b V_b^2 = \frac{1}{2} M_t V'^2_t + \frac{1}{2} M_b V'^2_b + E_t + E_b \quad (5)$$

Coefficient of Restitution

$$V'_t - V'_b = e(V_b - V_t) \quad (6)$$

One equation for ΔV of the target vehicle may be expressed by combining the above equations if the $F \Delta t$ term in the momentum equation is neglected:

$$\Delta V_t = \frac{(1+e)}{1 + \frac{m_t}{m_b}} \sqrt{\frac{2E(m_t + m_b)}{(1-e^2)m_t m_b}} \quad (7)$$

The relative approach velocity is

$$V_{RA} = \frac{1 + \frac{m_t}{m_b}}{(1+e)} \Delta V_t \quad (8)$$

Subscripts 't' and 'b' refer to 'target' and 'bullet'. Other nomenclature is as follows:

m	mass of vehicle
V	pre-impact velocity of vehicle centre of mass
V'	post-impact velocity of vehicle centre of mass
ΔV_t	velocity change of target
e	coefficient of restitution in vehicle-to-vehicle impact
E	energy absorbed by vehicles during collision
V_{RA}	Relative approach velocity

It is necessary to determine the coefficient of restitution for the vehicle-to-vehicle impact from the vehicle-to-barrier data. Howard et al⁹ discussed the coefficient of restitution for aligned impacts with low closing velocities. They present a derivation that yields the coefficient of restitution for a vehicle-to-vehicle impact from coefficient of restitution data from vehicle-to-barrier impacts involving the same vehicles.

$$e = \sqrt{1 + \frac{m_t(e_b^2 - 1) + m_b(e_t^2 - 1)}{m_t + m_b}} \quad (9)$$

where e_b and e_t are the bullet and target vehicle coefficients of restitution for barrier impacts.

The momentum-energy-restitution model was compared to the actual results for the VW-Ford test series. For the Volkswagen and Ford, the energy absorption and coefficient of restitution are shown in Figures 8 and 9 as functions of average isolator compression in vehicle-to-barrier impacts. Energy absorption is equal to the change in kinetic energy of the vehicle. It is assumed that most of the energy is absorbed by the isolators, though some is likely absorbed by the tires and suspension. This does not affect the empirical correlation between isolator compression and energy absorption.

The Volkswagen ΔV was predicted from the momentum-energy-restitution model as follows:

- For each vehicle-to-vehicle impact, note the average isolator compression on each vehicle
- From average isolator compression in a specific vehicle-to-vehicle impact, determine the energy absorbed and coefficient of restitution from vehicle-to-barrier data in Figure 8 (VW) and 9 (Ford)
- Determine the coefficient of restitution for a vehicle-to-vehicle impact from the coefficients of restitution in the vehicle-to-barrier impacts from Equation 9
- Determine ΔV for the vehicle-to-vehicle impact from Equation 7

Comparison of predicted and actual Volkswagen ΔV for the vehicle-to-vehicle impacts is shown in Table 1 and Figure 10.

Predicting Volkswagen ΔV from the vehicle-to-barrier data only (correlating ΔV with isolator compression) yields an overestimate if the VW data are used. If the compression of the bullet vehicle's front isolators are used, then the target vehicle's ΔV is underestimated. Using the momentum-energy-restitution model gives better agreement for this test series. In the vehicle-to-vehicle tests the predicted and actual restitution values are biased towards the higher Volkswagen value, except in the last vehicle-to-vehicle impact. In the last impact, the actual value is closer to the Ford vehicle-to-barrier value.

Using the vehicle-to-barrier isolator compression versus energy absorption correlation overestimated the energy absorption in all four of the vehicle-to-vehicle tests. In the last test the actual restitution was lower than predicted. In that test the bullet vehicle had an impact speed of 3.9 m/s, representing a kinetic energy of approximately 11400 Joules. Though the average isolator compression was lower than in the previous tests, the left VW isolator "bottomed out". Hence the actual change in kinetic energy probably included some energy that was absorbed in the vehicle structure, but not by the isolators. When the energy absorbed is larger than expected and the coefficient of restitution is lower, it is possible that the isolators' capabilities for energy absorption are exhausted and energy is being absorbed elsewhere (i.e. isolator or its mount is accumulating damage). In such cases, the vehicle-to-barrier data must be used cautiously.

As in the Ford / Volkswagen tests, it was found in a series of Ford Escort / Toyota Corolla tests that the energy absorption was higher for the isolator equipped Ford in vehicle-to-barrier tests than in vehicle-to-vehicle tests for the same amount of isolator

compression. The Ford Escort had bumper-mounted load cells at each front isolator. Compared to vehicle-to-barrier impacts, these vehicle-to-vehicle impacts had lower peak forces (Figure 11) and longer durations (vehicle-to-barrier = 125 ms, vehicle-to-vehicle = 175 ms) for the same amount of isolator compression. Hence the energy absorption is greater for a certain isolator compression in the barrier impact than in the vehicle-to-vehicle impact. It is known that the isolators are strain rate sensitive, which may explain the discrepancy. This strain rate sensitivity has not been explored for other vehicle-to-vehicle impacts. The reader should note the difference between the vehicle constitutive properties at these low speeds, and the strain rate independent relation $F=A+Bx$ which is applied at higher speeds. If these two test series represent a trend, then using barrier test data to estimate energy absorption will yield overestimates because of the difference in duration and the effect of strain rate.

If the effects of braking are accounted for by including the $F\Delta t$ term (impulse at wheels) then it is found that the ΔV of the struck (target) vehicle is reduced, and that of the striking (bullet) vehicle is increased (see Reference 3). In circumstances where braking is only minor, as in the case where the target vehicle operator is using the brakes only to hold the vehicle stationary, the effect of ignoring braking is negligible. When braking is significant, as may be the case for some vehicles in a multiple vehicle collision, then the effect of braking should be considered. For solution of the equations, it is most efficient to re-cast them with the left hand side of the momentum and restitution equations equal to zero, estimate V_b , and solve for V_b' and V_t' . Energy absorbed will be a function of the V 's. The initial V_b can be refined until the energy absorption correlates with the observed damage. Setting V_t to zero (or any arbitrary value) does not affect the resulting ΔV 's.

The influence of mass was investigated using two 1982 Ford Escorts. One Escort had a mass of 909 kg. It was in numerous front-end vehicle-to-barrier tests empty, and with 225 and 450 kg added. The second Escort had a mass of 995 kg. Vehicle-to-barrier data for frontal impacts are presented in Figures 13 to 16.

Each series of vehicle-to-barrier impacts in Figures 13 to 16 exhibits a characteristic increasing energy absorption and decreasing coefficient of restitution with increased isolator compression. At higher isolator compressions (but below a level where isolators or their mounts are damaged), the coefficient of restitution increases after decreasing. This

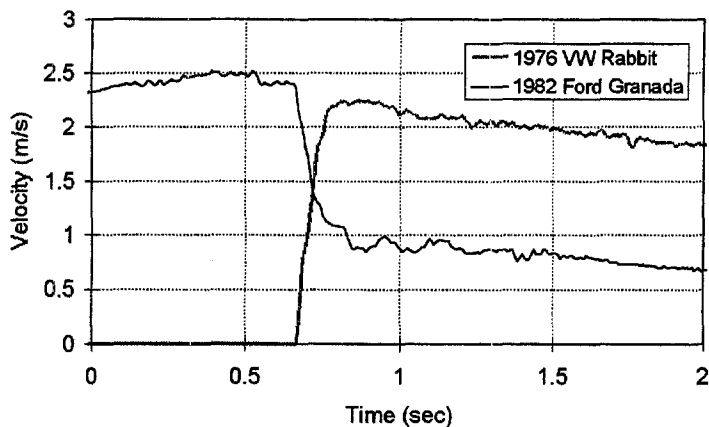


Figure 6. VW / Ford Granada collision speeds VW velocity change = 8.1 km/h.

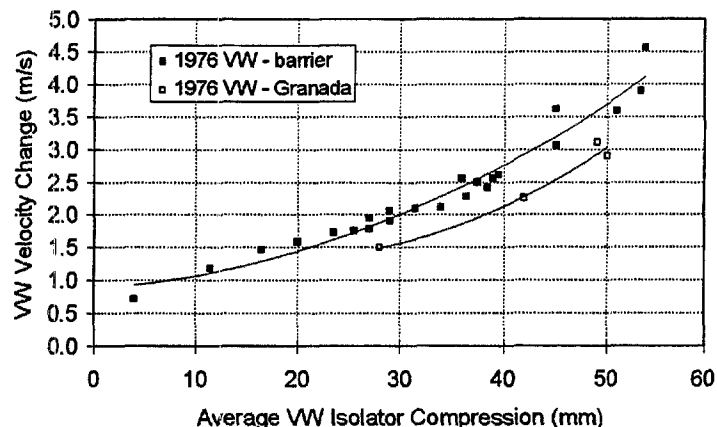


Figure 7. Average isolator compression, barrier and vehicle-to-vehicle impacts.

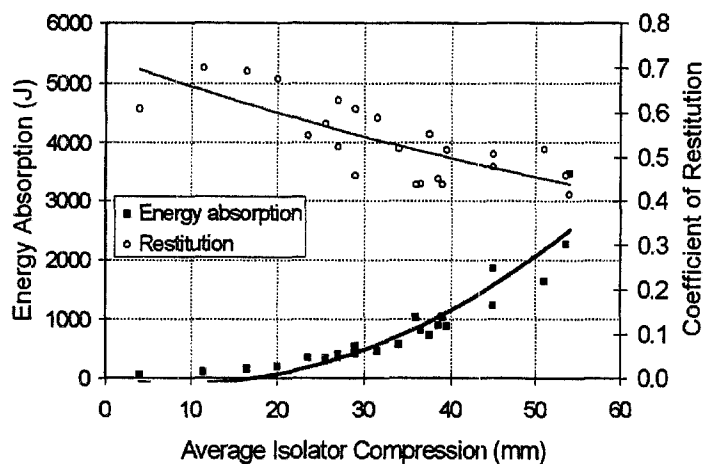


Figure 8. VW rear vehicle-to-barrier data.

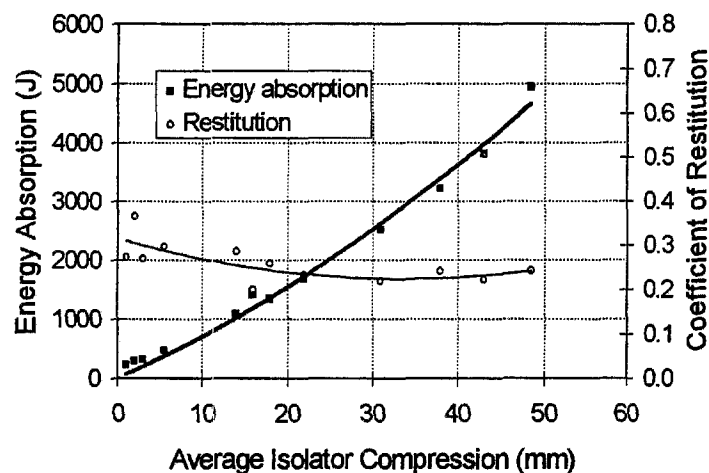


Figure 9. Granada front vehicle-to-barrier data.

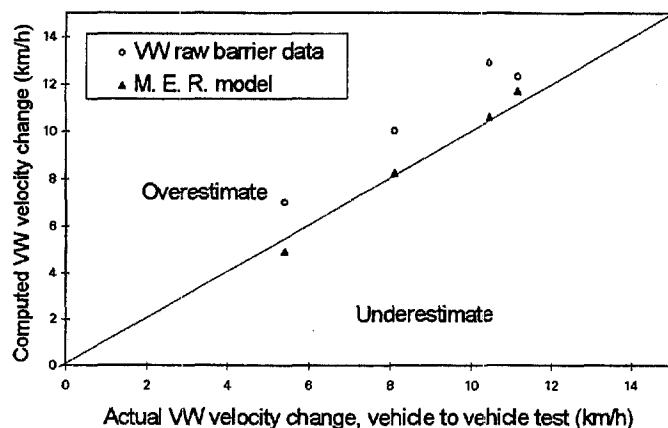


Figure 10. Actual and computed ΔV , vehicle-to-vehicle impacts.

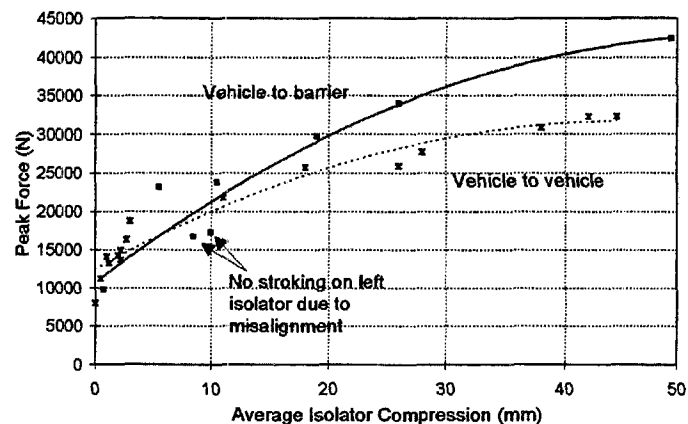


Figure 11. Escort front vehicle-to-barrier and vehicle-to-vehicle data.

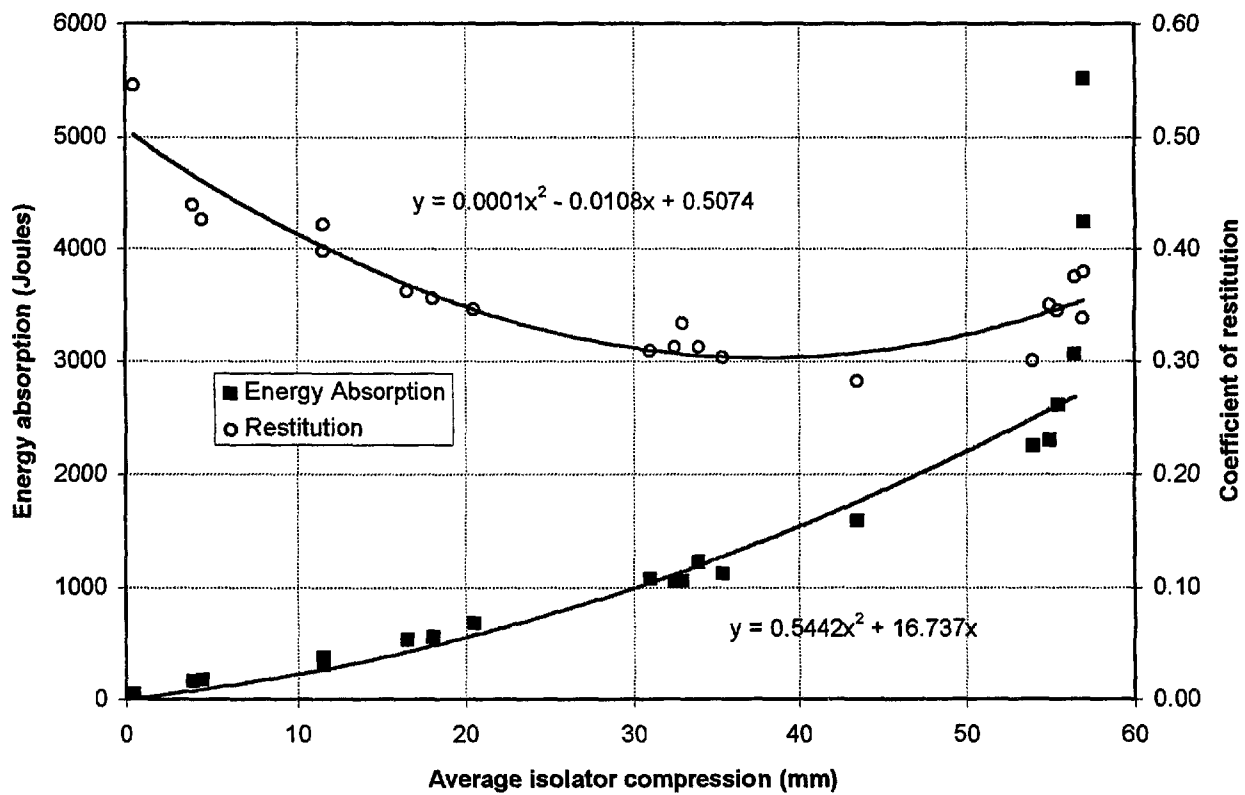


Figure 13. 1982 Ford Escort, empty (909 kg).

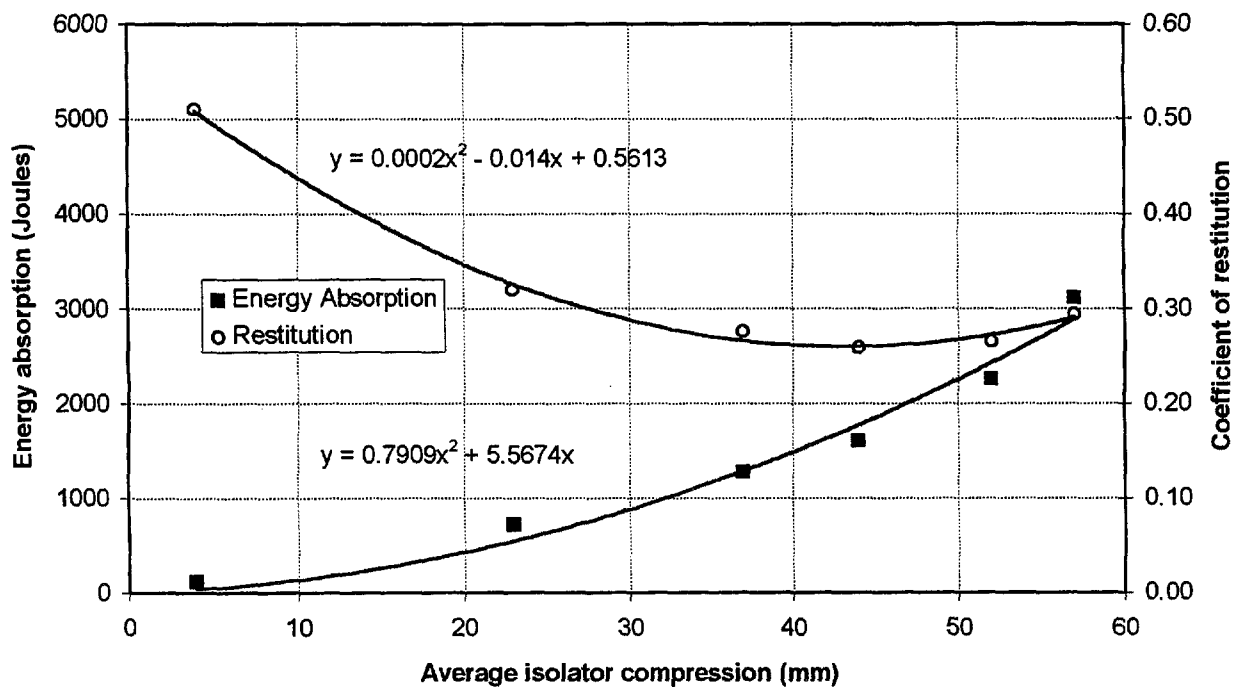


Figure 14. 1982 Ford Escort, 225 kg added (1134 kg).

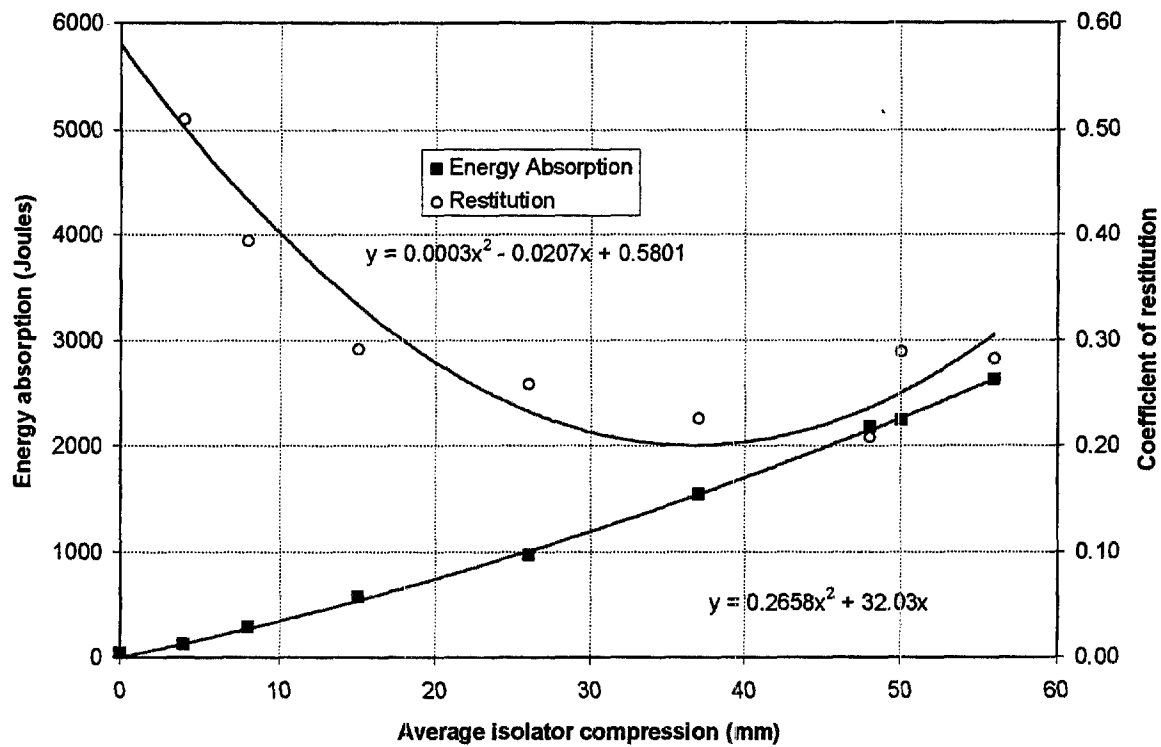


Figure 15. 1982 Ford Escort, 450 kg added (1359 kg).

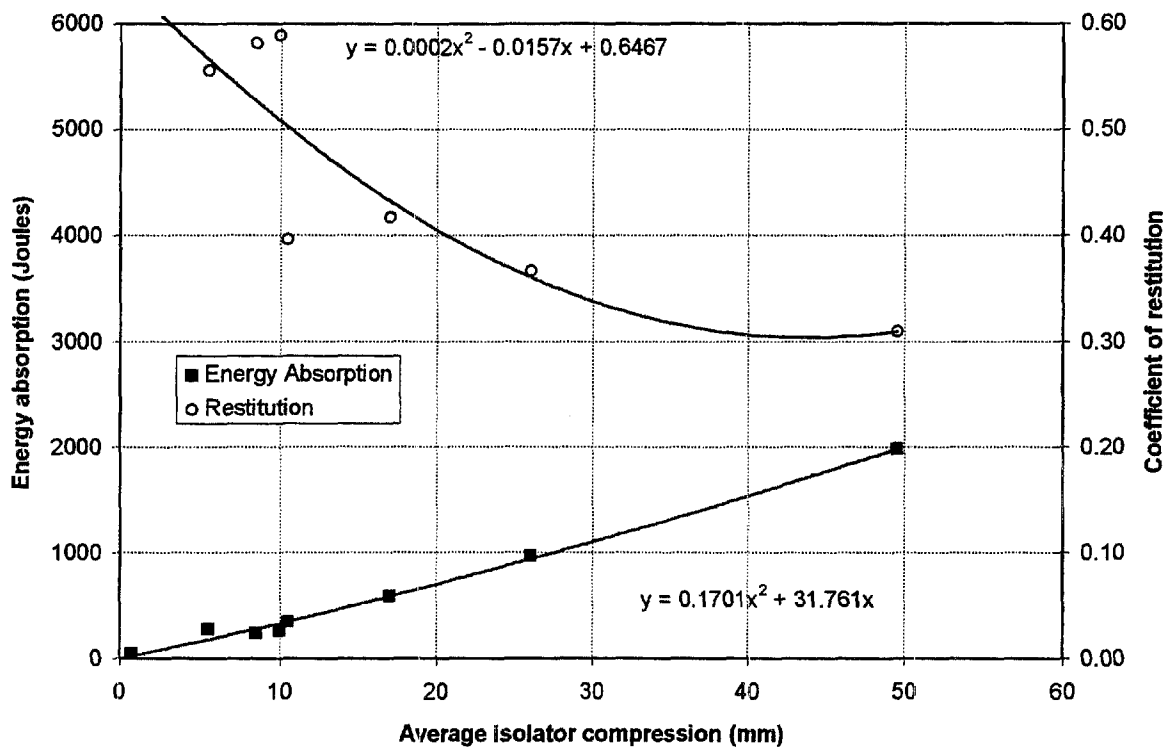


Figure 16. 1982 Ford Escort, Empty (995 kg)

Table 1. Volkswagen and Ford vehicle-to-barrier data for vehicle-to-vehicle tests.

VW avg. iso'r comp. (mm)	Ford avg. iso'r comp. (mm)	VW vehicle-to-barrier energy (J)	Ford vehicle-to-barrier energy (J)	Pred'd. Energy absorbed (J)	Actual Energy absorbed (J)	VW vehicle-to-barrier rest'n	Ford vehicle-to-barrier rest'n	Pred'd rest'n (Ref 9)	Actual rest'n	VW Pred'd ΔV (km/h)	VW Actual ΔV (km/h)
28	0	358	0	358	352	0.56	0.31	0.48	0.56	4.9	5.4
42	1.5	1284	65	1349	879	0.49	0.31	0.43	0.48	8.2	8.1
50	6	1980	407	2387	2153	0.47	0.28	0.41	0.42	10.6	10.4
49	10.5	2207	743	2950	2779	0.47	0.27	0.41	0.23	11.7	11.2

appears to be related to the isolators bottoming-out, and has been observed previously (see Reference 1). The restitution is lowest when the isolator is maximally compressed, but not bottomed-out. For the energy absorption curves, the constants in a quadratic curve fit $E=Ax^2+Bx$ (which ignores any effect of strain rate) and vehicle mass are tabulated below. The curves are forced to pass through the origin, indicating no energy absorption for no isolator compression.

Table 2. Ford Escort isolator comparison.

Mass (kg)	Coeff. A	Coeff. B
909	0.54	16.73
1134	0.79	5.56
1359	0.27	32.03
995	0.1701	31.761

For comparison, the Ford Granada had coefficients A and B of 0.78 and 74.68. The Volkswagen Rabbit values were 1.29 and -22.49. The quadratic relation appears to fit the data well, except for Figure 13. In that series of tests, the isolators began to bottom out. In Figure 13 the right-most three data points were exempted from the curve-fit.

There are many non-isolator equipped vehicles for which correlations between bumper isolator compression and ΔV or energy absorption cannot be made. Some vehicles with foam-core bumpers can withstand significant impacts, up to 14 km/h ΔV , without damage. The reader is referred to the authors' previous work for more details on different bumper types (Reference 2 and 3).

Limited data on foam core and rigid mount bumpers are available. Figure 17 shows energy

absorption and restitution as a function of peak force for a 1980 Toyota Corolla with a foam core bumper. The rear bumper contacted a rigid barrier with either its whole width, or was offset so that only 50% of its width made contact. No significant difference in energy absorption versus peak force was noted between the full contact and 50% offset tests. In both test types the average force, defined as $m\Delta V/\Delta t$, was approximately 41% of the peak force. If it was hit by a vehicle for which the peak or average force was known then the energy absorption of the foam core could be estimated. For example, if the other vehicle was isolator equipped, the average force $F=m\Delta V/\Delta t$ could be estimated by correlating its isolator compression with barrier test data. Alternatively, the peak force could be estimated from a dynamic test of the isolator(s). However, it would be inappropriate to use static isolator compression data.

Figure 18 shows energy absorption and restitution data for rigid mount steel bumpers from pick-up trucks and vans. The physical evidence for correlation is the permanent crush measured at six equally spaced points.

In some cases it may be possible to estimate ΔV from Equation 8 if reliable estimates of *approach velocity* are available. However, the *distance* a vehicle moved forward after an impact usually does not provide a reliable way to estimate closing speeds or speed changes. The distance a vehicle rolls forward after being hit depends on when and how hard the brakes were applied. Also, estimates of distance may also be unreliable. In one of the authors' demonstrations, spectators outside the vehicles viewed a vehicle-to-vehicle collision with a 4 km/h ΔV on both un-braked vehicles. Immediately

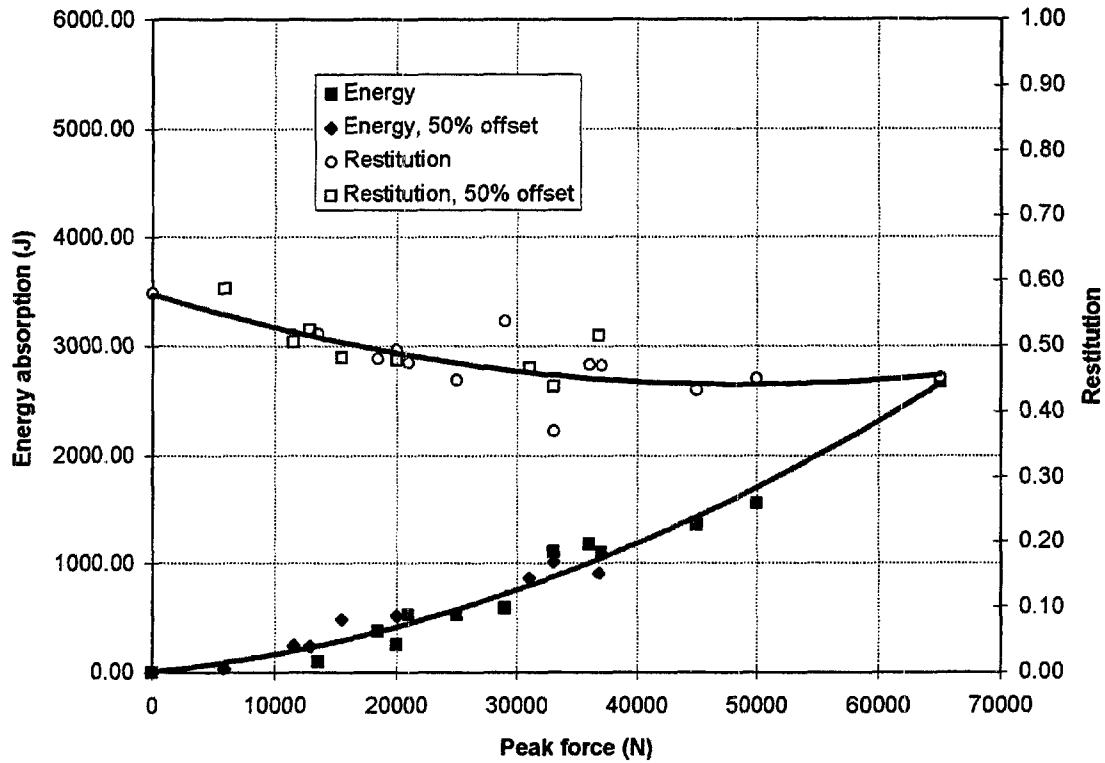


Figure 17. Toyota Corolla rear vehicle-to-barrier impacts.
(Average force, defined as $m\Delta V/\Delta t$, was $0.41F_{peak}$.)

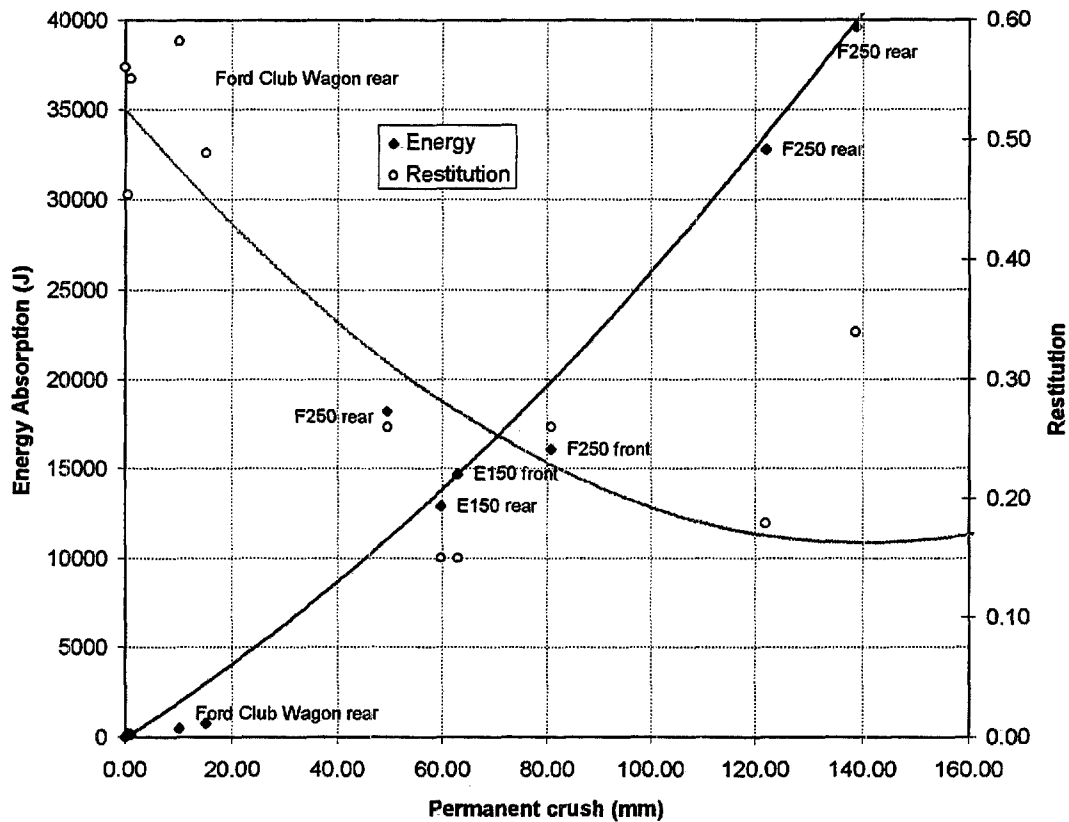


Figure 18. Rigid mount steel bumper vehicle-to-barrier impacts. E150 and F250 data from Woolley¹⁵.

after impact the vehicles were returned to their initial positions. Spectators were then asked to estimate how far the target vehicle rolled forward. Their responses are tabulated below. Less than one-third of the respondents were correct *immediately* after the impact.

Displacement interval	Respondents
0 to 5'	2
6 to 10'	6
11 to 15'	7
>15'	7 ← correct
Total = 22	

Below a certain ΔV , a vehicle in a rear-end or front-end collision is undamaged because of the protection afforded by its bumper. At higher ΔV 's, the damage threshold is reached, where structural damage starts to appear. From the data in Table 3a and 3b, the damage threshold is in the range 13 to 20 km/h ΔV for rear-end impacts and 10 to 17 km/h ΔV for front-end impacts. In some vehicle-to-vehicle tests it has been found that more damage is produced on the rear-ended target vehicle than on the bullet vehicle (see for example, Eubanks¹⁰). In Ford Escort vehicle-to-vehicle tests those authors found no damage on the front-ended Escort at approximately 20 km/h ΔV , and quarter panel buckling on the rear-ended Escort, which experienced nearly the same ΔV .

In the authors' experience, few of the passenger car bumpers tested were damaged after 8 km/h barrier impacts. These results may differ from results reported by other organizations, such as Consumer Reports or the Insurance Institute for Highway Safety, if the vehicles in those tests have different bumper designs. The results in this study apply to vehicles that met Canadian standard CMVSS 215. It is possible that some American vehicles have different bumper designs because they must pass a different standard.

VOLUNTEER EXPOSURES (FRONT, REAR-END). Human volunteer data in rear-end collisions come from staged collisions conducted by Severy¹¹, McConnell et al, Szabo et al¹², MacInnis Engineering, and from a study of amusement park bumper car collisions by Siegmund and Williamson¹³ (see Table 4). These data help to correlate impact severity with injury potential. In the tests, the impact severity is known with precision, and is empirically correlated with the volunteers' subjective evaluations of the effect the impacts had on them.

In the McConnell study, none of the volunteers had any symptoms below severities of 4 km/h ΔV . At severities in the 6.5 to 8.1 km/h ΔV range some of the male volunteers reported neck or back symptoms lasting for less than a day.

Male and female volunteers in the Szabo study experienced staged rear-end impacts, all at severities of 8 km/h ΔV . 4 of the 5 volunteers experienced transient headaches which resolved prior to exiting the vehicle and one of the female volunteers had minor transient neck stiffness. No additional symptoms were reported in the one year period following the tests.

In studies of amusement park bumper cars, no symptoms were reported by two male volunteers who endured rear impacts with severities up to the 7.7 km/h ΔV level. There were no head restraints in the bumper cars.

In rear-end collisions staged by MEA, there have been a number of male and female volunteers endure collisions with severities up to 8.8 km/h ΔV . The volunteers have expressed no concern or discomfort as a result of collisions with severities less than 4.3 km/h ΔV . The lowest severity where a volunteer has reported symptoms is at 5.8 km/h ΔV .

Comparing the above damage threshold data in Table 3a with the volunteer data in Table 4, it appears that neck and or back symptoms can occur in a rear-end impact without vehicle damage.

Human volunteer data for front-end impacts found in the literature (see Table 5), and tests done at MacInnis Engineering, suggest that front-end impacts have less potential for injury to seat-belted occupants than rear-end impacts at similar severity.

Chandler and Christian¹⁴ tested 18 male Air Force volunteers in staged frontal collisions. The volunteers were seated in an automotive bucket seat that was fitted with a lap and torso seat belt. The seat was propelled at approximately 24 km/h, then came to a 12g stop. Nine of the test subjects reported no indication of pain following the tests, one had clavicular and sternal pain and eight reported minor neck, back or chest pain or headaches.

Siegmund and Williamson measured the ΔV 's experienced by amusement park bumper cars. The bumper cars were equipped with loose fitting torso-only seat belts. During the tests, a 32 year old male experienced severities from 6.8 to 8.1 km/h ΔV during 7 staged frontal impacts, and a 25 year old male experienced severities of 7.1 to 8.1 km/h ΔV during 3 staged frontal impacts. All of the tests were conducted within a two hour period. Neither occupant reported any neck or back pain as a result of the impacts.

Table 3a . Rear-end damage threshold data.

Test	Vehicle	Velocity change (km/h)	Coeff. of restitution	Energy absorption (Joules)	Damage
492†	1980 Chevrolet Citation	13.6	0.29	4362	Isolator flange bent; quarter panel buckling
704	1977 Honda Civic	13.2	0.55	1475	Buckle in left quarter panel
851	1980 Toyota Tercel	13.0	0.47	2017	Right corner of bumper pushed forward
853	1980 Toyota Tercel	17.6	0.40	4435	Buckling of both quarter panels and trunk floor; bumper cover puckered
388	1981 Ford Escort	16.5	0.31	5134	Buckling of both quarter panels
Woolley ¹⁵	1979 Pontiac Grand Prix	16.1	0.27	9138	3.6 cm crush
	1978 Honda Accord	17.8	0.14	9117	Buckling of both quarter panels; 4.3 cm crush
	1983 Ford T-bird	18.9	0.12	17515	7.4 cm crush
	1980 Chevrolet citation	19.9	0.28	9256	7.1 cm crush
	1979 ford E-150 van	16.1	0.15	12865	6.1 cm crush
	1979 Ford F250	19.6	0.20	18817	4.8 cm crush; bumper rotated clockwise viewed from left

Table 3b. Front-end damage threshold data.

Test	Vehicle	Velocity change (km/h)	Coeff. of restitution	Energy absorption (Joules)	Damage
834†	1987 Ford Tempo	8.3	0.39	1245	Left isolator stuck in
515	1980 Chevrolet Citation	10.8	0.26	2945	Broken spot welds at front of frame
360	1981 Ford Escort	10.9	0.30	2297	Mild flattening of bumper
441	1979 Chevrolet Malibu	11.5	0.28	3370	Flattening of bumper; left end of bumper rotated clockwise viewed from left
362	1981 Ford Escort	13.9	0.38	3133	Isolator flange damage
683	1981 Dodge Aries	14.2	0.27	4679	Bumper flattened and bulging of cover at ends
329	1978 VW Rabbit	15.2	0.52	2444	Bumper bent up slightly
627	1976 Volvo	17.4	0.38	7555	Isolator pushed back
162	1986 Chevrolet Cavalier	11.7	0.30	3031	Bumper beam bent

† MacInnis Engineering test number

Table 4. Human volunteers in staged rear-end collisions.

Vehicle	Subject	Speed Change (km/h)	Symptoms	Source
1947 Plymouth	Male	8.7, 9.3	none	Severy
1984 GMC pick-up	45 to 56 year old males in good physical condition	3.04	"...considered later by the participating physician test subjects to have been so very mild that a single exposure would have been unlikely to have resulted in any symptomatology."	McConnell et al
1984 Ford van		3.48		
1984 Buick Regal		3.93		
1984 Ford van		6.45	twinge at base of neck 45 min post test, 2h duration	
1984 Ford van		6.61	sore neck 1 day post test, 5h duration	
1984 GMC pick-up		7.03	none	
1984 Buick Regal		7.83	sore neck 1 day post test, 5h duration	
1986 Dodge 600 convertible		8.06	mid back and neck discomfort, 1 day post test, 1 day duration	
1976 VW Rabbit	Males	5.3, 5.8, 5.9, 6.4, 6.8, 7.6, 8.3, 8.6, 8.8	none, except pain at back of head from contact with headrest at 8.8	MEA tests
1977 Chevrolet Caprice	Male	3.7, 3.8, 4.4, 6.3, 7.0, 8.8	none, except for twinge in neck and brief dizziness at 7.0 and moderate short term neck stiffness after all six tests	
1980 Toyota Corolla	Females	2.3, 2.9, 3.0, 3.1, 3.2	none	
1980 Toyota Corolla	Males	1.7, 2.3, 2.7, 2.9, 3.0, 3.0, 3.0, 3.0, 3.2, 3.3, 3.6, 3.6, 4.2	none	
1984 Toyota Tercel	Male	6.3, 7.9	headache after 7.9	
1984 Toyota Tercel	Female	3.1, 4.4, 5.8	headache after 5.8	
1986 Chevrolet Cavalier	Male	3.5, 3.7, 3.8, 3.8, 4.1, 4.1, 4.2, 4.3, 4.3	none	
1991 Nissan pick-up	Males	2.1, 2.6, 3.5, 4.6, 5.0	none	
1987 VW GTI	Male	3.3	none	
Honda Accord	Males	4.0, 5.5, 5.5, 5.5, 6.2, 6.9	none	
PNE bumper cars	2 Males	5.8, 6.4, 6.9, 7.0, 7.2, 7.6, 7.6, 7.7	none	Siegmund and Williamson
1981 and 1982 Ford Escort	27 year old female	2 impacts "approx, 8"	transient headache immediately post-impact which resolved spontaneously and transient minor neck stiffness the morning after the test	Szabo et al
	48 year old male	"approx, 8"	transient headache immediately post-impact which resolved spontaneously	
	58 year old female			
	31 year old male			
	28 year old male	"approx. 8"	none	

Table 5. Human volunteers in staged front-end collisions.

Vehicle	Subject	Velocity Change (km/h)	Symptoms	Source
1941 Plymouth	Male	10.5, 11.9, 11.6, 23.8	none	Severy
1981 Dodge Aries	Male	10.0	none	MEA tests
1982 Ford Granada	Male	8.5 10.0, 10.4, 12.7	none	
1983 Pontiac Gran Prix	2 Males	7.5, 8.1	none	
1990 Plymouth Sundance	Male	3.6, 3.8	none	
Daisy accelerator, Holloman AFB impact sled	Eighteen male volunteers (20 to 32 year old male air force personnel)	21.3, 22.4, 22.5, 22.6, 22.8, 22.9, 23.5, 23.6, 23.6, 23.6, 23.8, 23.8, 23.8, 23.8, 23.9, 23.9, 24.0, 24.0, 25.7	9 subjects: none 8 subjects: neck pains of moderate severity. 1 subject: moderately severe clavicular and sternal pain.	Chandler and Christian
Naval Air Development Centre Horizontal Accel'r	Navy personnel	16 to 20 km/h	Minor neck pain "ouch" level	Glenn
Wham I impact sled	Male restrained by a lap belt and two criss-crossing shoulder belts.	12 to 24 km/h	Neck and back pains lasting for several days with 1.4 kg (3 lb) weight on head for a velocity change of 24 km/h. No injuries for a velocity change of 23 km/h without weight on head.	Mertz and Patrick
Modified WHAM II impact sled	17 U.S. Army personnel in 236 tests.	Up to 50 km/h (Maximum peak sled acceleration of 9.9 g)	No reported injuries except minor abrasions. All returned to duty immediately.	Ewing and Thomas
Bumper cars	2 Males	6.1, 6.8, 7.0, 7.2, 7.1, 8.1, 7.9, 8.1, 8.1	None	Siegmund and Williamson

In other testing involving Navy personnel reported by Glenn¹⁶, subjects reported minor neck pain (which the author referred to as the "'ouch' level") at impact speeds of 16 and 20 km/h with decelerations of 8.2 to 11.3g. Higher severity tests were conducted, but the subjects had their heads tucked forward. One test was conducted at 48.9 km/h and was 'injury free'. Mertz and Patrick¹⁷ studied the flexion response of a fiftieth percentile male volunteer. The volunteer was seated and restrained with a lap belt and two criss-crossing shoulder belts. The seat was accelerated to speeds of 12 to 24 km/h, then stopped at 2 to 9.6g. The volunteer experienced a total of 46 impacts. In the 24 km/h impact the volunteer experienced pain in

his neck and back for a number of days. In that particular impact the volunteer had a 3 lb. weight attached to the top of his head. The volunteer went on to experience impacts after this up to 23 km/h, but without additional head weights, and experienced no adverse effects.

Ewing and Thomas¹⁸ subjected 17 volunteers from the U.S. Army to a total of 236 frontal impacts. The volunteers wore a lap belt, 'inverted V' shoulder harness and chest safety strap. No injuries were reported at impact speeds up to 50 km/h and 9.9g deceleration.

LATERAL COLLISIONS

Lateral collisions were staged using the Ford Granada, Ford Escort and Toyota Corolla. The test matrix is shown in Table 6.

Table 6. Lateral collision vehicle engagements.

Test	Target	Bullet
1	1980 Toyota Corolla right fender	1980 Ford Granada front
2	1980 Toyota Corolla right front door	1980 Ford Granada front
3	1980 Toyota right B-pillar	1980 Ford Granada front
4	1980 Toyota Corolla right doors	1980 Ford Granada front
18*	1980 Toyota Corolla right quarter panel	1982 Ford Escort front
19	1980 Toyota Corolla right quarter panel	1982 Ford Escort front
20	1980 Toyota Corolla right quarter panel	1982 Ford Escort front
21	1980 Toyota Corolla right rear door	1982 Ford Escort front

* test numbers 5 to 17 used for unrelated experiments

The vehicles' masses and front/rear mass distributions were measured using a pair of 10000 lb (44500 N) load cells placed first under one axle, then the other. Table 7 shows the masses and their distribution.

Table 7. Vehicle masses for lateral tests.

Vehicle	Mass (kg)	Dist'n F/R
1980 Toyota Corolla	977	56/44
1980 Ford Granada	1282	56/44
1982 Ford Escort	995	64/36

In Tests 1 and 2, both vehicles were in motion and aligned at 90°. The front bumper of the Ford Granada hit the right front wheel of the Toyota in the first test, and the right front door in the second test.

In Test 1 the right front wheel of the Toyota was bent inward at the top. Starting at the front bumper, there was a 109 cm long contact mark on the Toyota from the Ford that reached a maximum depth of 11 cm and tapered to zero at the ends. The impact changed the Toyota's heading by 25° counterclockwise. Figure 19 shows the Ford initial speed was approximately 12 km/h and its ΔV was approximately 7.5 km/h. The Toyota, which was initially moving forward approximately 18 km/h,

slowed to zero in about 600 ms, an average deceleration (without braking) of about 0.85g. The Toyota lateral acceleration (measured at near centre of mass on transmission tunnel) peaked at about 4.8g. There was no direct measurement of lateral ΔV . It was estimated to be 6.8 km/h using Equations 10 to 13 (later in this section), with known values from the test for damage location, V_b , ΔV_b and Δt . The total change in kinetic energy was approximately 2500 Joules.

In Test 2 there was a 95 cm long contact mark on the right front door that reached a maximum depth of 9 cm. The right front window was rolled down prior to the impact, and shattered as a result of the impact. Even though the window was down, glass fragments were found inside and outside the vehicle. The impact changed the Toyota's heading by 10° clockwise. This rotation was the opposite direction from the previous test because the impact force was directed aft of the Toyota centre of mass. Figure 20 shows the Ford initial speed was approximately 11.5 km/h and its ΔV was approximately 7.2 km/h. The Toyota was initially moving forward at approximately 9 km/h and slowed to zero in about 800 ms, an average deceleration of about 0.32g. The Toyota lateral acceleration peaked at about 4g. The lateral ΔV was estimated to be approximately 6.2 km/h using equations 10 to 13. The total change in kinetic energy was approximately 3895 Joules.

In both these tests the volunteer Toyota driver moved toward the right relative to the vehicle, as expected. The driver did not hit any part of the vehicle interior. The lateral velocity went from zero to its peak and back to zero quickly. This differs from a rear-end or front-end impact where the velocity goes from its initial value to its peak, but not back to its initial value. In the lateral impacts, the occupant is not forced to "catch-up" with the car, as he would have to in the rear-end or front-end types of impacts. There were no severe neck loads because the volunteer's upper body pivoted toward the right about the lap belt resulting in little displacement of the head relative to the torso.

In Tests 3 and 4 the target Toyota was stationary and the impact was concentrated over the right doors and B-pillar. Some of the damage was superimposed over damage from test 2. In Test 3 (Figure 21) there was very slight crush to the B-pillar and a small lateral displacement. The Ford frontal ΔV was 3.5 km/h. The Toyota lateral acceleration had several peaks of less than 1g with pulse widths less than 20 ms. In the more severe Test 4 (Figure 22) there was approximately 40 mm of crush to the B-pillar, the front and rear axles moved sideways 280 and 500 mm, and there was bumper contact across both right side doors. The Ford frontal ΔV was 5.4 km/h. The

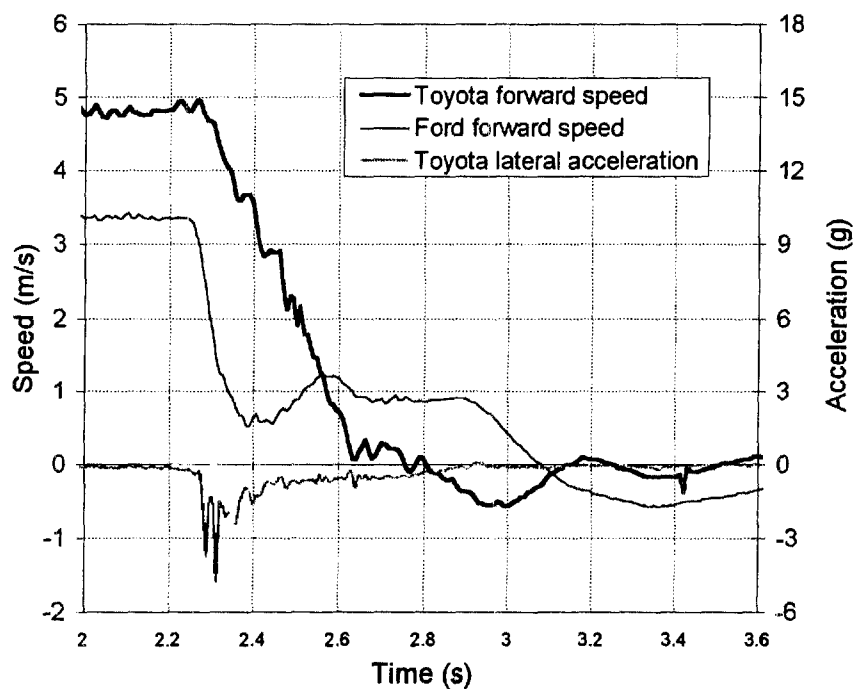


Figure 19. Speed and acceleration for test 1. Damage to right fender.

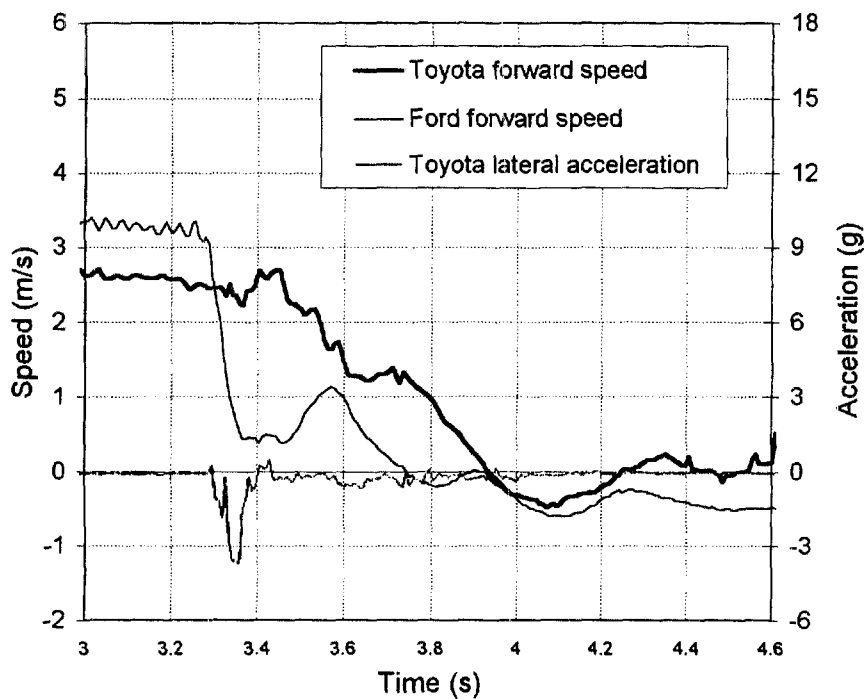
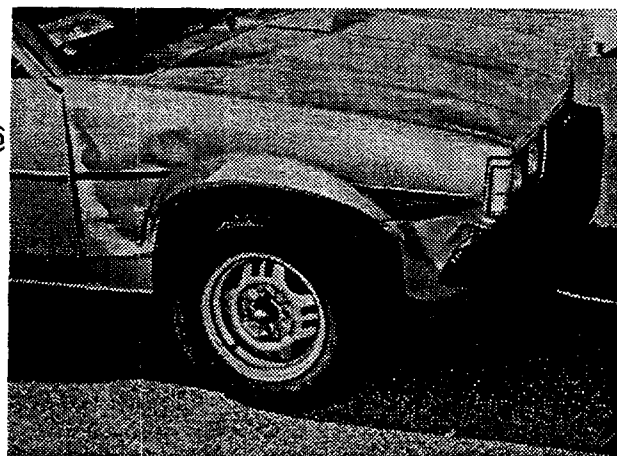
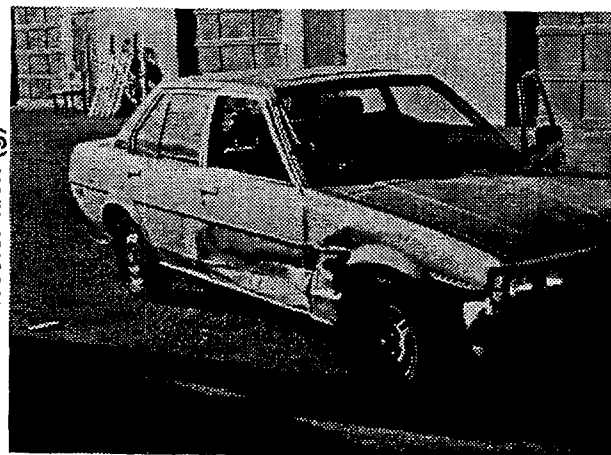


Figure 20. Speed and acceleration for test 2. New damage to right front door. Old damage to right fender from test 1.



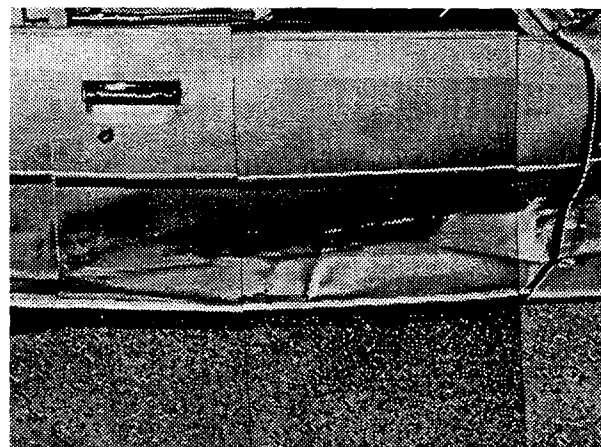
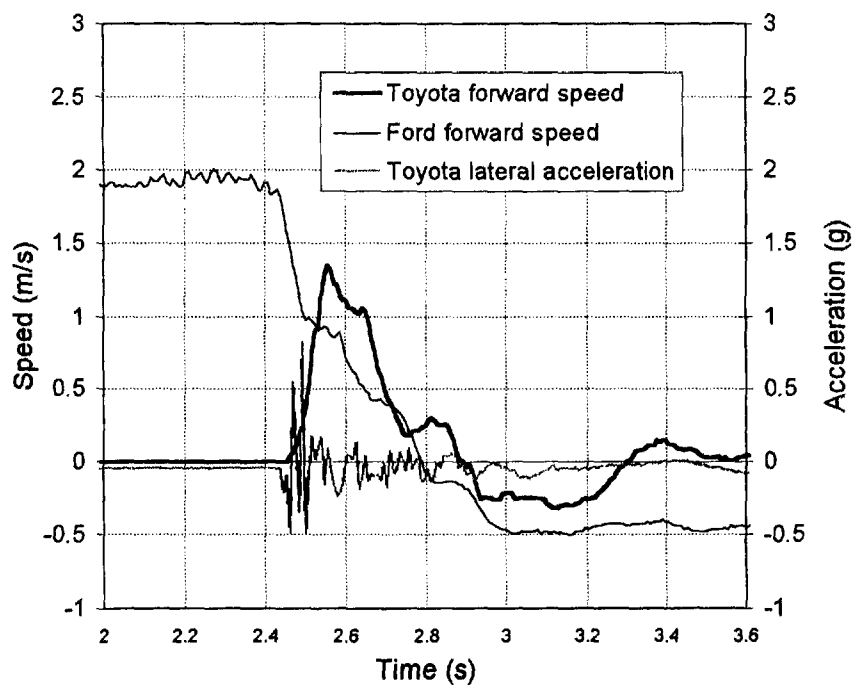


Figure 21. Speed and acceleration for test 3. Additional damage to lower right front door. Same area was damaged in test 2.

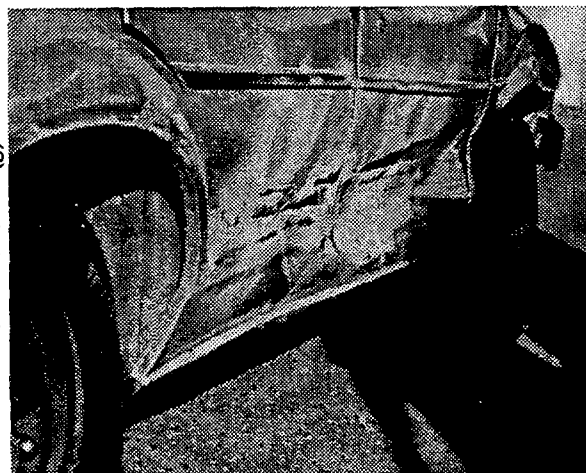
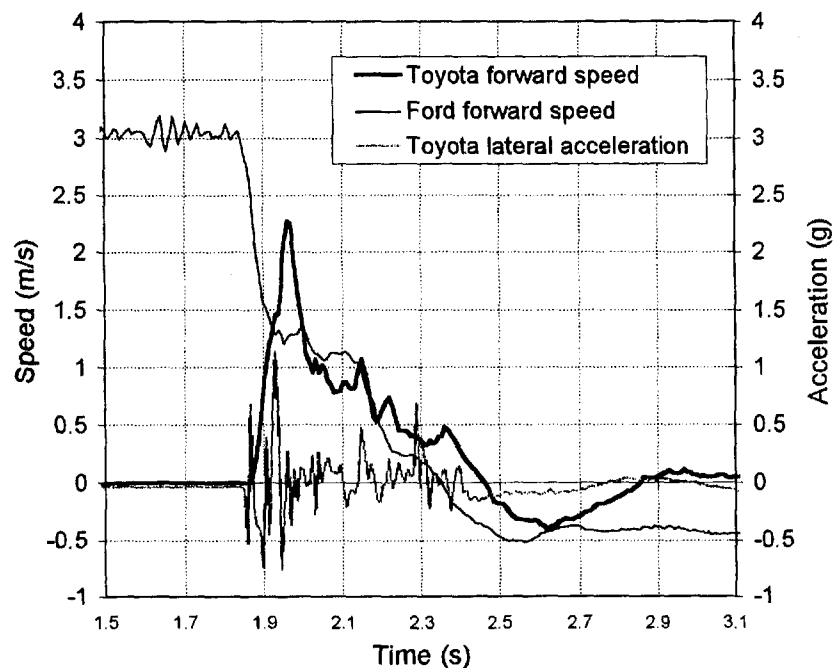


Figure 22. Speed and acceleration for test 4. Damage right rear door and B-pillar.

Toyota lateral acceleration had a 1g peak with a 40 ms pulse width above a background of other sub-1g peaks of lesser pulse duration.

In Tests 18 to 21. The vehicles were aligned at 90°, with the left front corner of the Ford aligned with the right rear corner of the Toyota (Figure 23).



Figure 23. Vehicle engagement in tests 18 to 21.

In Test 18 the top of the left bumperette of the bullet Ford Escort hit the target Toyota Corolla right quarter panel aft of the rear wheel. There was no damage or isolator compression on the Ford, and a dimple in the quarter panel of the Toyota that was 50 mm in diameter and a maximum of 5 mm deep. Vertical scuffs on the 50 mm height of the damage indicated the Toyota had displaced vertically by approximately 50 mm at the contact point. In these tests, generally the bullet front bumper pitched downward slightly and the struck side of the target rolled upward. The wheels of the Toyota did not slide sideways as a result of the impact.

Figure 24 shows that the bullet Ford was moving at 1.44 km/h at impact. It decelerated as the rear of the target Toyota accelerated sideways. The target rear end reached its peak lateral velocity of 0.5 m/s about 100 ms after impact and became stationary 125 ms after initial contact. The load cell data show the force between the vehicles reached zero about 100 ms post-impact. After the 100 ms, the Ford ΔV was approximately 0.2 m/s. Because the target wheels were sideways on the road surface and the bullet vehicle was free to roll, the bullet vehicle pressed on the target vehicle a second time as the target vehicle velocity dropped below that of the bullet vehicle. About 300 ms after the initial contact the bullet vehicle rebounded backward off the target vehicle. The lateral acceleration of the target vehicle top and bottom was in phase, and had a 0.7g peak with a 10 ms pulse width at the roof. The total change in kinetic energy during the impact was approximately 33 Joules.

In Test 19 the engagement was identical to Test 18, but the closing speed was higher. The dent was at the same location on the target Toyota, only it was 200 mm in diameter and 18 mm deep at the centre and centred 301 cm from the front axle. There was also a small scrape on the rear of the right rear wheel arch of the Toyota from the bumper of the Ford. Neither of the Ford isolators compressed. The rear bumper of the target vehicle displaced sideways 19 cm relative to the ground. Figure 25 shows that the closing speed of the bullet Ford was approximately 1.4 m/s. After the first 100 ms the force between the vehicles dropped to zero. Unlike the previous test, the target vehicle slid sideways, so the bullet rolled ahead until it contacted it a second time and decelerated with it, but with very little force between the vehicles. Eventually the bullet vehicle disengaged and rolled away backwards. The ΔV 's at the Ford and Toyota centres of mass were approximately 0.8 and 0.5 m/s and the change in kinetic energy pre- and post-impact was approximately 438 Joules. 321 Joules were accounted for by the sliding tires, and the remaining 116 Joules were associated with the damage to the Toyota. The roof-top acceleration had a 2.3g peak with a 12 ms pulse width above a background of lower peaks that lasted a total of 100 ms.

In Test 20 the alignment was similar to the two previous tests, but the closing speed was high enough to cause 2 and 13 mm compression on the left and right Ford isolators. The target Toyota rear bumper moved 45 cm sideways relative to the ground. The front axle did not move sideways. The portion of the right quarter panel that was hit in the previous test was hit again in this test, causing the dent to increase in size. The dent was centred 290 cm from the front axle (11 cm closer). There was some new damage ahead of the target Toyota right rear wheel arch that was 6 cm in height, 4 cm in length and approximately 1 cm in depth. Figure 26 shows that the dynamics were similar to the previous test. The impact lasted approximately 100 ms, then the force between the vehicles dropped to near zero and then the vehicles decelerated in unison. The peak force at the bumper of the bullet was approximately 25 kN for an average isolator compression of 7.5 mm (front-end vehicle-to-barrier impact: peak force=24 kN, isolator compression=7.5 mm). The change in kinetic energy pre- and post-impact was approximately 1092 Joules. 569 Joules were associated with isolator compression and work done by the sliding tires, and 523 were associated with the Toyota damage. The top accelerometer measured a 3.5g peak with pulse duration of 10 ms above a background of lower peaks.

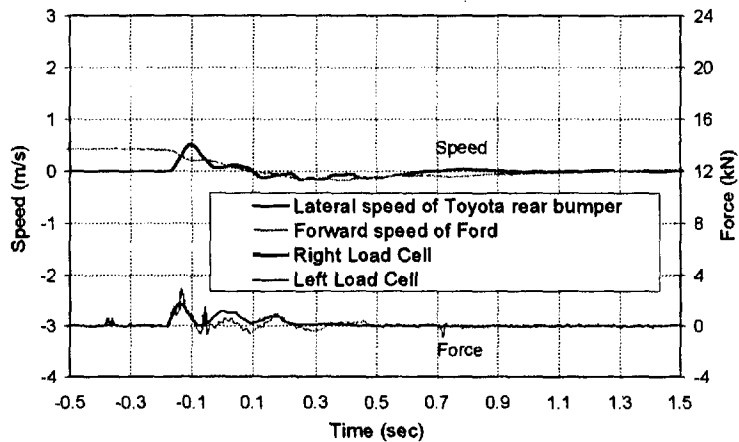
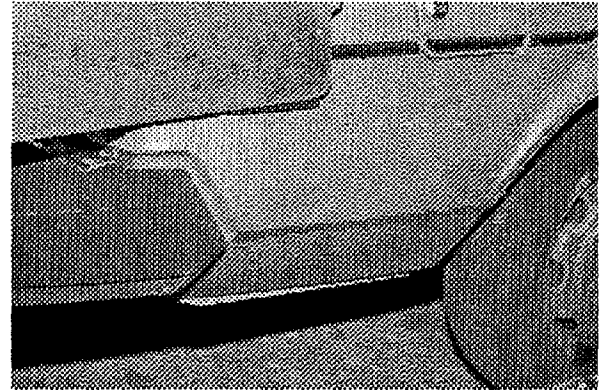


Figure 24. Speed and force data, test 18. Damage shown at right



Small dimple in quarter panel from Ford bumperette.

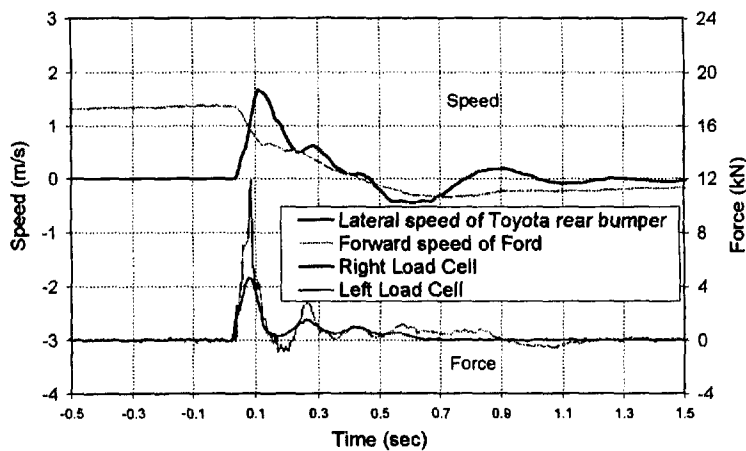
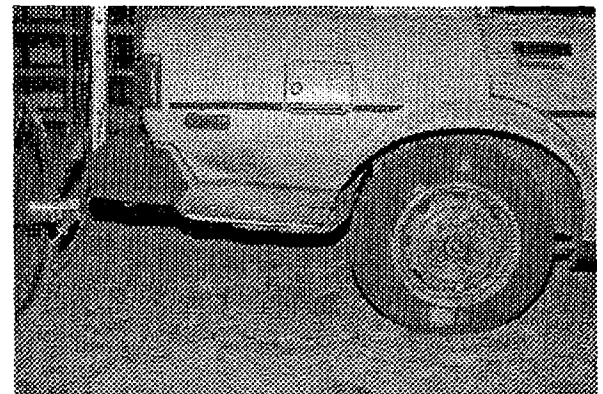


Figure 25. Speed and force data, test 19. Damage shown at right.



Dent in quarter panel, 200 mm diameter, 18 mm maximum depth.

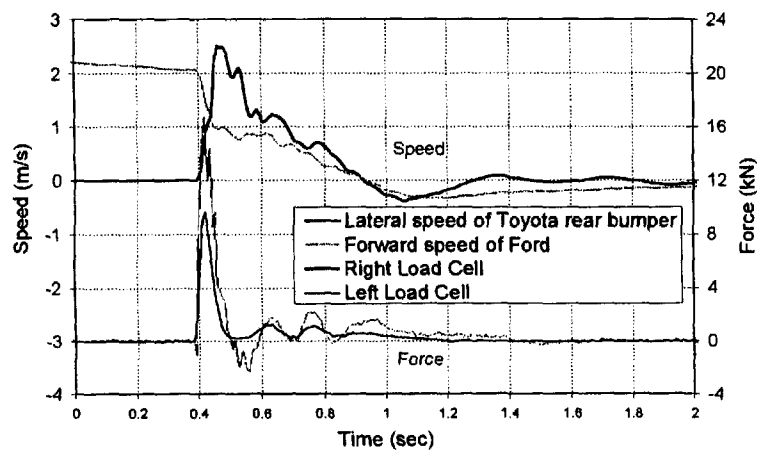


Figure 26. Speed and force data for test 20. Damage shown at right.



Dent in quarter panel 11 cm farther forward than test 19, plus small dent in wheel arch leading edge.

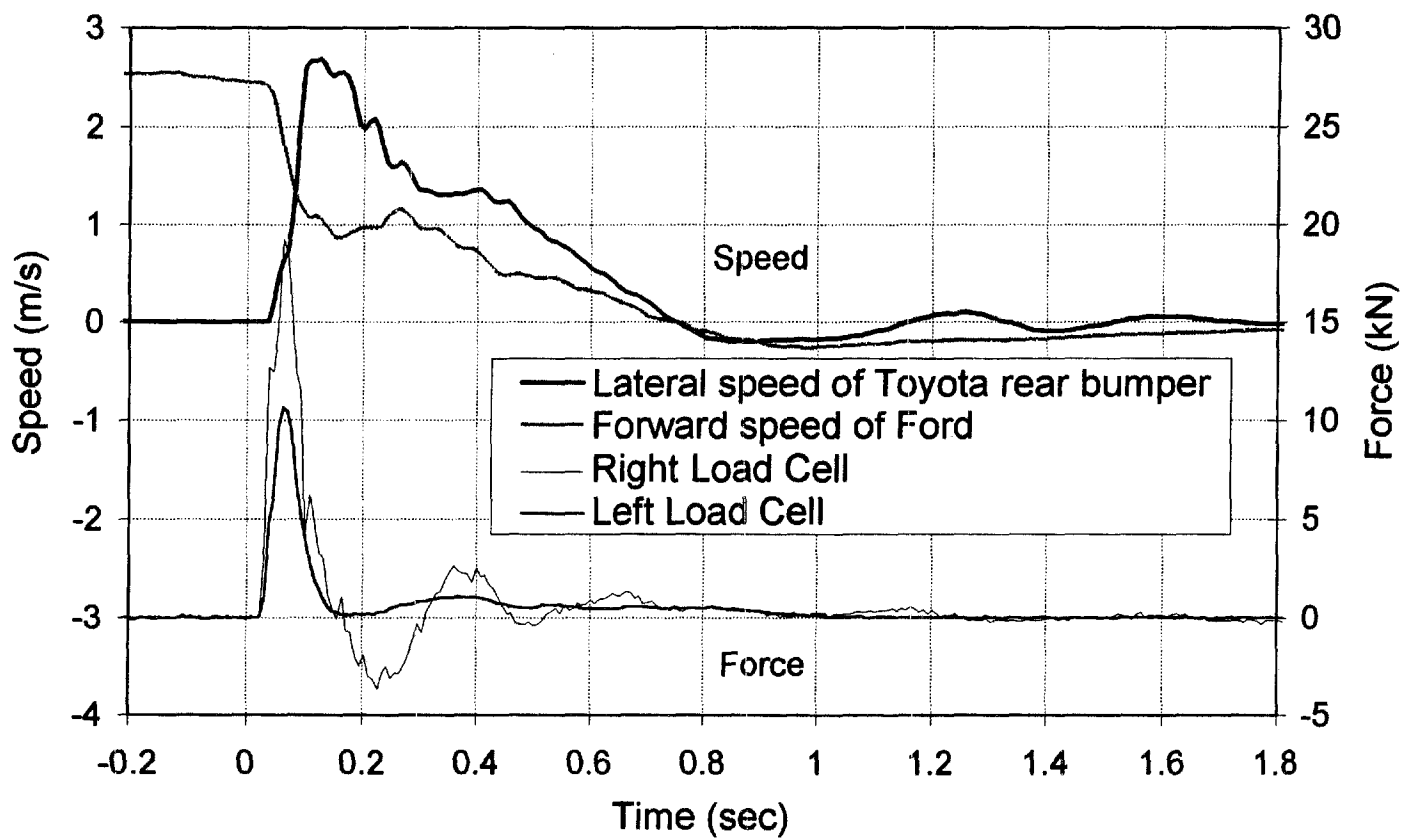


Figure 27 (a). Speed and force data for test 21.

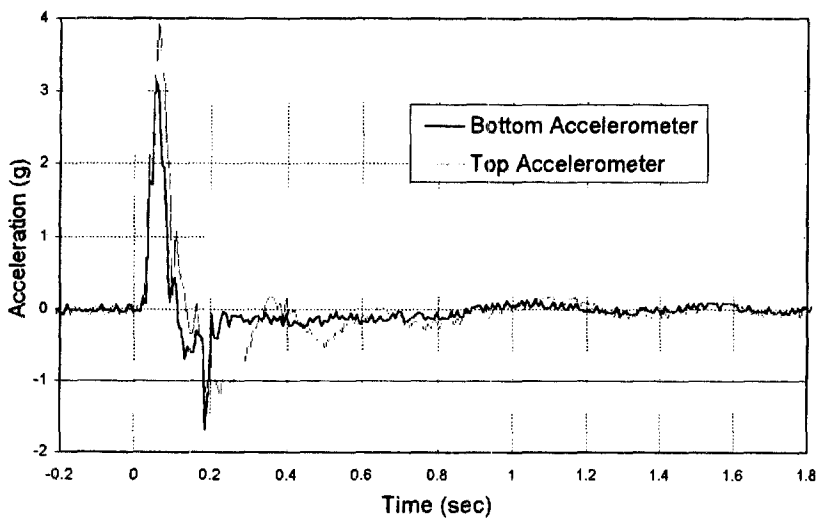
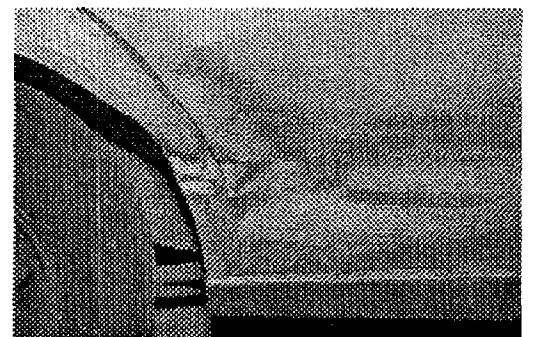
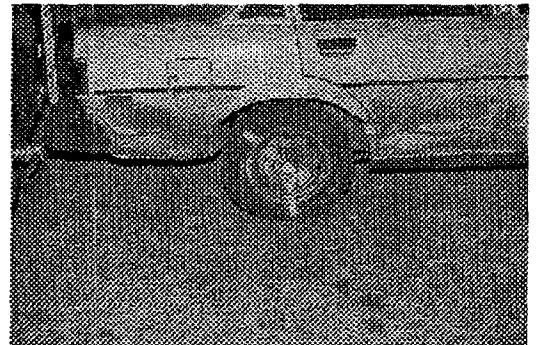


Figure 27 (b). Acceleration at transmission tunnel and roof for test 21. Damage shown at right.



In Test 21 the alignment was similar to the three previous tests, but the bullet Ford was slightly more forward. The impact speed was 8.6 km/h. On the Toyota there was a 16 cm long dent in the rear door approximately 20 mm deep. There was a black scuff in the dent that went forward and downward. It was caused by the motion of the Toyota relative to the Ford, which was upward and backward. The dent in the Toyota right rear wheel arch had doubled in depth to 2 cm. There was 7 and 20 mm compression on the left and right Ford isolators. The target Toyota rear bumper moved 79 cm sideways relative to the ground and the front axle did not move. Figure 27 (a) shows that the dynamics are again similar to the previous tests. The change in kinetic energy pre- and post-impact was approximately 1638 Joules. The energy absorption associated with the 13.5 mm average compression is 460 Joules. 733 Joules were associated with the Toyota damage. The top accelerometer measured a 4g peak with a 110 ms pulse width (Figure 27 (b)).

SEVERITY PREDICTION (LATERAL). Like the momentum-energy-restitution model for rear-end or front-end impacts, similar principles can be applied to derive a similar model for lateral impacts. In this model, conservation of angular momentum must be introduced and the impulse term $F\Delta t$ must be included in the momentum equations (except in very slippery road conditions). The model applies to lateral impacts where the front or rear axle of the target acts as a pivot, i.e. there is no lateral displacement of one axle. The engagement and nomenclature are shown in Figure 28. The momentum, energy and restitution equations are as follows:

Conservation of Linear Momentum.

$$M_b V_b = M_t V'_t + M_b V'_b + F_t \Delta t \quad (10)$$

Conservation of Angular Momentum

$$M_b V_b r_3 = M_b V'_b r_3 + M_t V'_t r_1 + I_t \omega'_t + F_t \Delta t r_2 \quad (11)$$

Conservation of Energy

$$\frac{1}{2} M_b V_b^2 = \frac{1}{2} M_t V'^2_t + \frac{1}{2} I_t \omega'^2_t + \frac{1}{2} M_b V'^2_b + E_t + E_b + E_w \quad (12)$$

Coefficient of Restitution

$$V_b = e(\omega'_t r_3 - V'_b) \quad (13)$$

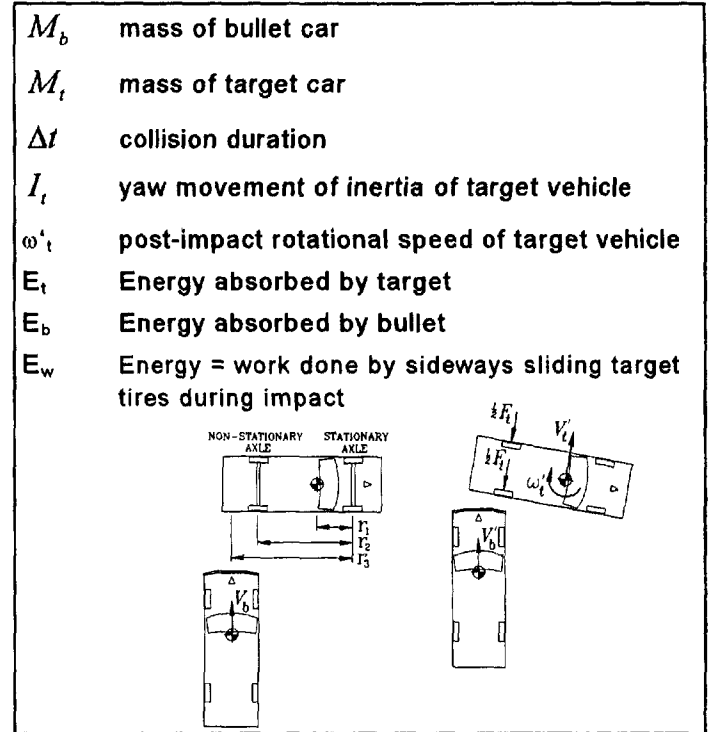


Figure 28. Nomenclature for lateral collision model.

The actual results for impacts 18, 19, 20 and 21 were compared to results predicted by the model. Input to the model included approach speed of the Ford, effective location of force application (determined from the Ford bumper-mounted load cells), impact duration, coefficient of restitution, road surface friction coefficient for sliding tires, vehicle masses, target Toyota yaw moment of inertia¹⁹, target vehicle wheelbase and target vehicle centre of mass to front axle distance. Output from the model included target and bullet ΔV , target vehicle $\Delta \omega$, and energy absorbed during impact. The results (shown in Table 9 as $\Delta \omega$ and energy absorbed) compared favorably, indicating the validity of the equations. However, some of the inputs, notably restitution and duration, were not available until after inspection of the test data. It appears that durations of approximately 100 ms and restitution values in the 0.2 to 0.6 range, typical for bumpers, are also appropriate for these impacts.

For a real impact, where the only physical evidence is vehicle damage, the investigator must record the location of damage, relate the amount of damage to energy absorption, then solve the above equations by selecting the bullet vehicle pre-impact velocity until the energy absorption value is reached.

Energy absorption values can be determined for the bullet vehicle if it is isolator equipped, from barrier test data. Energy absorption values can be determined for the target vehicle from the damage to its side, but data are scarce. For the tests presented here, the energy absorption of the side of the target was determined by subtracting from the measured change in kinetic energy as shown in Table 10.

Table 9. Comparison of actual and predicted results for tests 18 to 21.

Test	Δt (ms)	rest'n	$\Delta\omega_{\text{actual}}$ (r/s)	$\Delta\omega_{\text{predicted}}$ (r/s)	E_{actual} (Joules)	$E_{\text{predicted}}$ (Joules)
18	90	0.48	0.15	0.06	75	33
19	100	0.37	0.45	0.42	533	437
20	80	0.35	0.69	0.69	1107	1092
21	90	0.20	0.73	0.73	1651	1638

Table 10. Energy absorbed by target.

Test	ΔKE (Joules)	Isolator energy absorption + work done by sliding tires (Joules)	Energy absorbed by target (Joules)
18	33	0	33
19	437	321	116
20	1092	569	523
21	1638	905	733

For comparison, door impacts from two lateral collisions on a 1981 Chevrolet Malibu are shown in Figures 29 and 30. Constitutive relations for door panel damage found in Reference 20 predict the energy absorptions indicated.

VOLUNTEER EXPOSURES (LATERAL). Staged collisions where volunteers have participated in the vehicle struck laterally are listed below (Table 11).

In the MEA vehicle-to-vehicle tests, the lateral velocity of the target vehicle went from steady state to

peak (as a result of collision) then back to steady state (as a result of tire friction in the sliding direction) rapidly. The motion of the vehicle was lateral, there was no significant rotational displacement. The highest ΔV was 6.8 km/h. Peak accelerations were up to 4.8g and the impact durations were approximately 100 ms. The volunteers were seated in the driver's seat and the impact came from the driver's right side. The volunteers did not strike anything in the vehicle interior. No symptoms were reported by the male volunteers.

In a study by Zabrowski²¹, 37 male Air Force volunteers were subjected to a total of 70 lateral impacts. Volunteers were lap belted into a seat that was propelled left side leading at a speed of 15 to 17 km/h, then stopped suddenly. The seat had a side plate angled outward from the left side at 30° from vertical to prevent excessive flexion. From the impact speed the seat was stopped with a special brake at 4g, 6g, 8g or 10g peak acceleration levels. This was accomplished by varying the stopping distance (and time). Impacts at the 4g level had durations of over 300 ms, too long to be comparable to a lateral vehicle impact. At the 6, 8 and 10g levels the impact durations were 139, 103 and 100 ms for the sled in the lateral direction for the acceleration-time traces given for representative impacts. These durations are

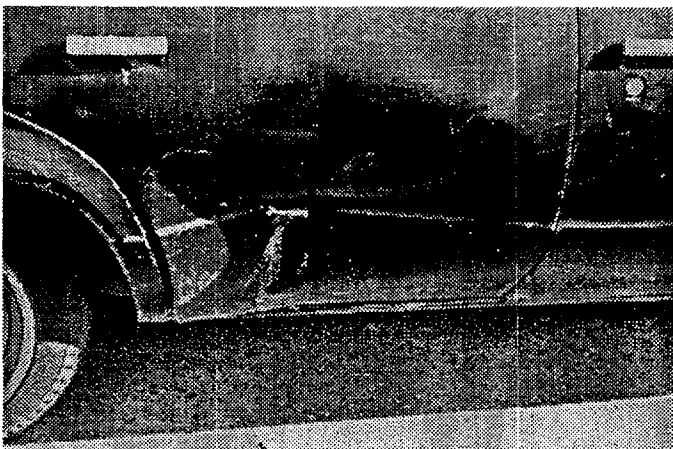


Figure 29. Chevrolet Malibu lateral impact. Energy absorption by door was approximately 400 Joules. Dent is 64 mm deep.

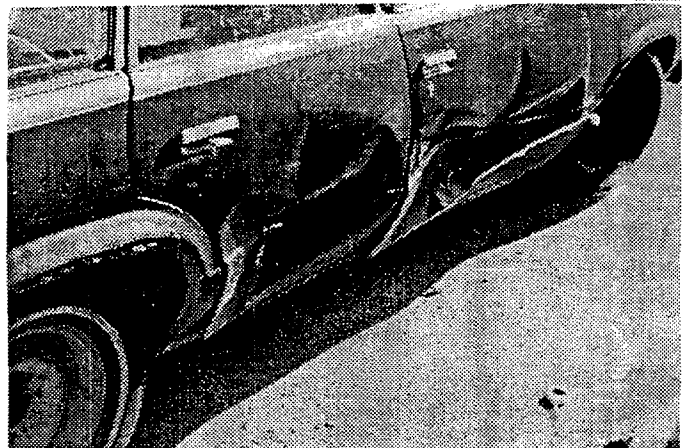


Figure 30. Chevrolet Malibu lateral impact. Energy absorption by door was approximately 900 Joules (forward door). Dent is 102 mm deep.

comparable to vehicle lateral impacts, and the 15 to 17 km/h sled velocity can be likened to a 15 to 17 km/h ΔV in a lateral impact.

No permanent physiological changes were noted in any of the volunteers. Half of the subjects had minor symptoms in testing above the 6g level. The symptoms resolved within days and were mostly head aches, neck, shoulder or hip pain. At the higher acceleration levels some brief disorientation was noted by some subjects immediately post-test. Many subjects felt no effects immediately post-test, but did

feel symptoms some hours later. Two subjects were very relaxed on impact. Both hit their heads on the side plate. One was unconscious for two minutes and the other had a head ache for 5 minutes. The subjects who were not as relaxed in many cases were able to avoid striking their heads on the side plate. There were no head strikes at the 4g level. Head to side plate strikes were recorded for 20% of the volunteers at the 6g level, 40% at the 8g level, and 50% at the 10g level.

Table 11. Human volunteers in staged lateral collisions.

Vehicle	Subject	Velocity Change (km/h)	Peak lateral vehicle acceleration (g)	Symptoms	Source
1980 Toyota Corolla	32 yr male	6.2, 6.8	4, 3.5	none	tests 1,2
1980 Toyota Corolla	26 yr male	0.7, 2.4, 3.7	0.4, 1.5, 3.6	none	tests 18, 19, 20
"Bopper" sled	24 yr male	17.2	5.79	pain in lower spine, < 1h	Zaborowski
	22 yr male	16.5	7.06	blow to head/shoulder; stiff R. neck 3 days, sore hips 2 days	
	28 yr male	16.6	6.38	sore R neck, 1 day delay to onset, 24h duration	
	31 yr male	16.0	6.64	sore neck, 1 day delay to onset, 24h duration	
	22 yr male	16.2	6.4	pain R hip, gone after exit from sled	
	31 yr male	16.6	5.77	none	
	24 yr male	16.8	6.43	burning sensation from seat belt	
	22 yr male	16.9	7.85	pain in hip bone "quickly subsided"	
	23 yr male	17.4	8.83	hit head, unconscious 2 min.	
	26 yr male	15.8	7.52	head hit shoulder; head ache 2h	
	37 yr male	17.7	8.48	stunned momentarily; stiff R neck	
	28 yr male	17.4	-	sore R neck, 8h delay to onset, <24h duration	
	29 yr male	16.5	7.55	very mild hip pain	
	23 yr male	17.4	8.16	burning sensation in hips; head barely touched restraint	
	24 yr male	16.8	8.09	mild belt bruising; sore R neck and R shoulder, 24h delay to onset	
	42 yr male	16.9	8.28	numb L arm; tired feeling	
	22 yr male	17.5	8.43	sore R neck, 3h delay to onset, 48h duration	
	24 yr male	15.8	8.9	mild momentary pain across under chin and across neck	
	21 yr male	16.6	9.95	R neck and R shoulder stiff for 3 days	
	26 yr male	15.8	9.32	dull ache in back of head, <1h duration	
	24 yr male	16.2	8.48	blurred vision for 10 sec, tired feeling	
	22 yr male	16.7	9.24	disoriented; head ache 6h duration; pain in neck and L trapezious 3 day duration	
	20 yr male	16.6	9.44	head ache 30 min duration; stiff neck 2h delay to onset, 12h duration	
	26 yr male	15.7	8.83	head ache 1h; sore R neck 3 days	
	31 yr male	17.4	8.83	stiff R neck and R trapezious, 18 hour delay to onset	
	25 yr male	15.0	9.14	head ache, 30 min delay to onset, 15 min duration	

SIDE-SWIPE COLLISIONS

Tests have been conducted to simulate side-swipe vehicle accidents. Side-swipes are generally impacts where the angle between the vehicles is shallow and a common velocity is not reached. Vehicle orientations and impact speeds were varied to investigate their influence on damage and impact severity. Test conditions are summarized in Table 12.

For all of the tests, a stationary target vehicle was placed in the path of a moving bullet vehicle. The target vehicle was positioned so that its longitudinal axis was at a small angle to the path of the bullet vehicle, and so that a corner of the bullet vehicle's front bumper would contact the side of the target vehicle.

The bullet vehicle was fitted with a 5th wheel. The target vehicle was fitted with either a 5th wheel (oriented longitudinally) and two accelerometers (both oriented laterally), or two accelerometers (one oriented longitudinally, the other laterally). In three tests there were two bumper mounted load cells in the bullet vehicle.

FORD ESCORT AND TOYOTA COROLLA TESTS. Three side swipe impacts (Tests 22, 23 and 24) were staged by pushing a Ford Escort into a Toyota Corolla. These tests followed lateral tests 18 to 21, and used the same instrumentation. The vehicles were oriented so that the right corner of the Ford front bumper would contact the left side of the Toyota when pushed straight ahead as illustrated in Figure 31. The transmission of the target vehicle was placed in neutral and no brakes were applied.

The bullet vehicle was equipped with a 5th wheel and bumper mounted load cells. The target vehicle had one accelerometer mounted to the floor pan at the centre line, just behind the front seats, and another on the roof directly above the first. Both accelerometers were oriented to measure lateral accelerations, i.e. perpendicular to the longitudinal axis of the vehicle. An MEA 5th wheel was fitted to the rear bumper of the target vehicle, parallel to the longitudinal axis.

For test 22, the Corolla was oriented at 10° to the path of the Escort and positioned so that the right corner of the Escort front bumper would contact its left front door. Velocity, force and damage are shown in Figure 32. As a result of the impact, there was a black mark running from a point 42 cm behind the leading edge of the left front door forward to the left front wheel. The mark was slightly higher at the beginning of contact than at the end of contact. As in the lateral tests, the mark has a downward orientation

because the target vehicle surface being struck has a tendency to rotate upward as a result of the lateral force applied to its side. The fine details of the material deposited on the side of the Toyota at this mark were obliterated because the cars were stuck together after impact; when they were pulled apart the surfaces scraped past each other for a second time. There was a slight dent in the Corolla door skin at the leading edge of the door. There was also a minor amount of material transferred to the Toyota driver's door from the Ford right front wheel arch. The Escort came to rest in contact with the Corolla. At rest, the Corolla had moved ahead 45 cm from its pre-impact location. The Escort's rest position was 128 cm ahead of its position at initial contact with the Corolla. The left load cell recorded almost no load, as expected. The right load cell peaked at approximately 700 N. The 977 kg Toyota experienced an average forward acceleration of less than 0.1g for the first 1000 ms of contact, then decelerated at approximately the same rate to rest. A total "velocity change" of 1.5 km/h occurred during the 1000 ms contact interval.

For test 23, the Corolla was oriented at an angle of 16° to the path of the Escort and positioned so that the right corner of the Escort's front bumper would contact its left front door. Velocity, force and damage are shown in Figure 33. The impact produced a black scrape mark running from the back of the Corolla's left front door to a point 45 cm behind the leading edge of the door. The scrape mark was associated with a dent in the door skin that had a maximum depth of 40 mm. Again, the scrape mark ended lower than it began, by about 4 cm. During the impact, both vehicles came to rest and then moved backwards. The Corolla came to rest behind its original position. The vehicles were not in contact when they came to rest. The left and right load cells both recorded compressive loads for the initial phase of the impact. After the vehicles were engaged, the right load cell recorded a tensile load which correspond to a slowing of the target vehicle. The right load cell peaked at approximately 1600 N.

For test 24, the Corolla was oriented at an angle of 16° to the path of the Escort and positioned so that the right corner of the Escort's front bumper would contact its left front door. Velocity, force and damage are shown in Figure 34. The impact produced a black scrape mark on the middle of the Corolla's left front door and fender. Denting of the door skin was not significantly increased over that due to previous impacts. The right corner of the Escort bumper became lodged behind the left front wheel of the Corolla, and the two vehicles came to rest in contact.

Table 12. Side-swipe tests.

Test	Target	Bullet	Angle	Approach speed (km/h)
SS8	Honda Civic left side	Dodge Aries right front	shallow	23.8
SS10	Honda Civic left side	Dodge Aries right front	shallow	25.9
SS11	Honda Civic left side	Dodge Aries right front	shallow	27.0
SS12	Honda Civic left side	Dodge Aries right front	shallow	8.6
SS13	Honda Civic left side	Dodge Aries right front	shallow	8.3
SS17	Honda Civic right side	Dodge Aries left front	shallow	19.1
SS18	Honda Civic right side	Dodge Aries left front	shallow	19.8
SS19	Honda Civic right side	Dodge Aries left front	$\approx 30^\circ$	20.2
22	Toyota Corolla left side	Ford Escort right front	10°	4.5
23	Toyota Corolla left side	Ford Escort right front	16°	5.0
24	Toyota Corolla left side	Ford Escort right front	16°	9.4

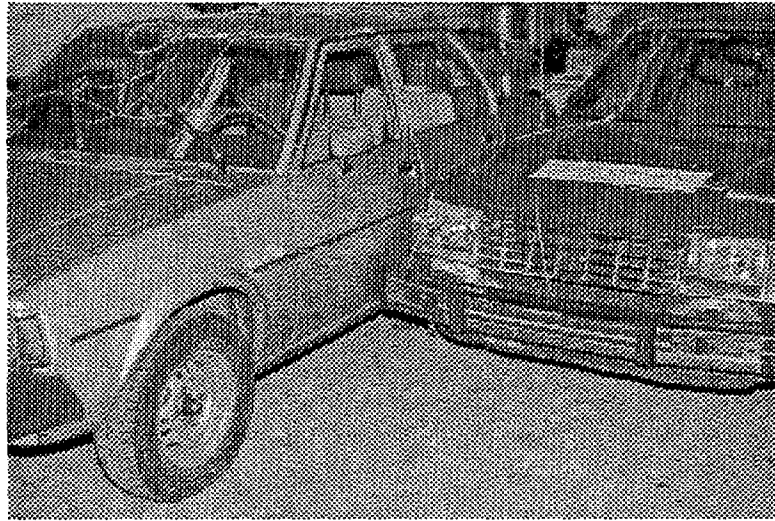


Figure 31. Vehicle engagement for side-swipe tests.

DODGE ARIES AND HONDA CIVIC TESTS. Eight side swipe impacts were staged by propelling a Dodge Aries into a Honda Civic. The vehicles were oriented so that a front corner of the Dodge would contact the right or left side of the Honda. The Dodge approached the Honda from the rear in all tests. The transmission of the target vehicle was placed in neutral and no brakes were applied for tests SS8, SS10, SS11, SS12 and SS13. In tests SS17, SS18

and SS19 the transmission of the Honda was in second gear and no braking was applied.

For all tests the disturbance of the Honda was observed to last approximately 1.5 to 2 seconds and the acceleration data were judged to be periodic. The acceleration data, acquired at 200 Hz, were filtered to include only the part of the spectrum below 80 Hz. The test results are summarized in Table 13.

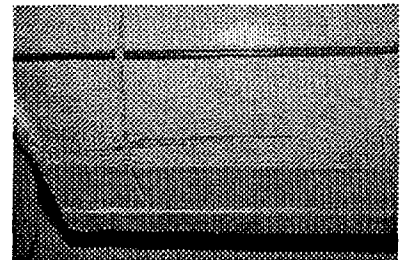
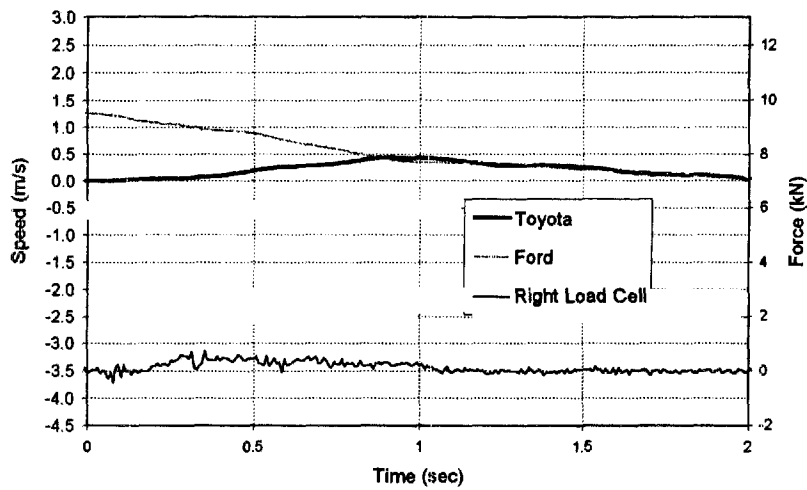


Figure 32. Speed and force for test 22. Damage at right.

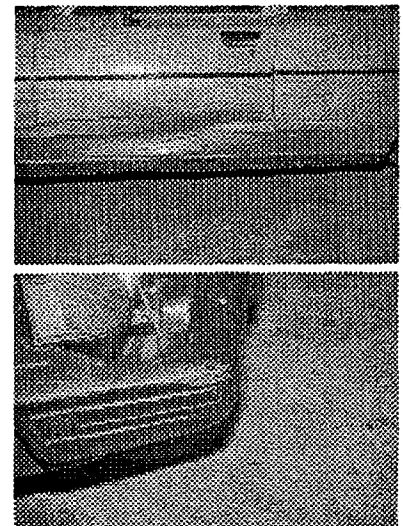
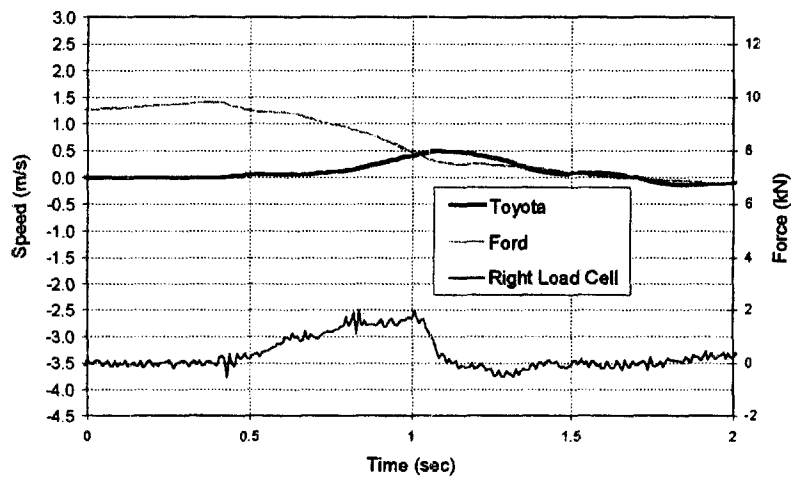


Figure 33. Speed and force for test 23. Damage at right.

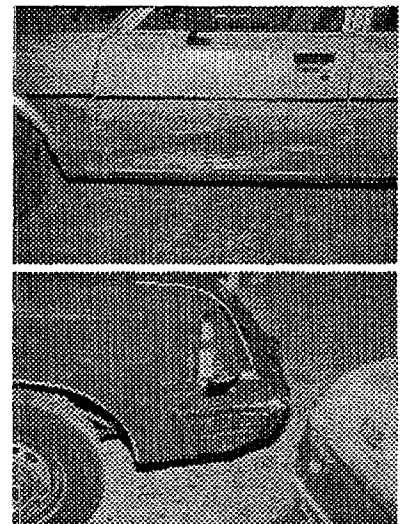
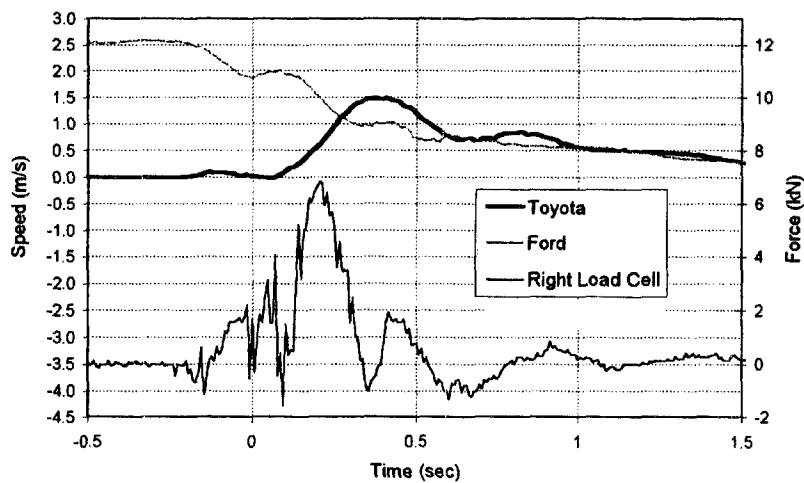


Figure 34. Speed and force for test 24. Damage at right.

Table 13. Summary of Dodge / Honda side-swipe tests.

Test	Fig	Damage	a_{long}		a_{lat}		Δt (ms)
			peak (g)	pulse width	peak (g)	pulse width	
SS8	35	The Dodge snagged the left front corner of the Honda, pulling the front bumper from the left isolator, and causing some left fender damage in front of the wheel well. Lateral movement was damped to zero in under one second. A black mark was left along the right door and quarter panel of the Honda. The Dodge did not slow considerably during the impact. The left front wheel of the Honda moved to the right 5 cm and the vehicle moved ahead 3 cm as a result of the collision.	4.0	30 ms	0.5	150 ms	900
SS10	36	The right front corner of the Dodge caught the left front wheel well of the Honda, causing fender damage on both sides of the wheel arch. The Dodge was not brought to rest by the impact.	2.0	150	1.0	150	1000
SS11	37	Initial contact occurred with the right corner of the Dodge front bumper snagging the trailing edge of the Honda left fender. The rear attachments of the fender were broken and the fender was dented above the wheel arch. The Dodge was not brought to rest by the impact. The initial snag caused a brief 5g longitudinal acceleration on the Honda. This was followed shortly by secondary contact that caused a 1.8g longitudinal and lateral acceleration of greater duration.	5.0	30	1.8	150	750
SS12	38	Right corner of the Dodge struck the left door of the Honda just in front of the B-pillar. Damage to the Honda consisted of horizontal scrape marks down the length of the left door. The Dodge came to rest in contact with the Honda as a result of the impact.	1.0	300	0.8	100	1000
SS13	39	Initial contact behind the B-pillar and more pronounced denting of the door skin as well as a dent in the left quarter panel. The Dodge came to rest as a result of the impact, in contact with the Honda. The damage was similar to the previous test.	1.4	30	0.5	150	1400
SS17	40	Initial contact occurred with the left corner of the Dodge front bumper striking the right door of the Honda, about 30 cm behind the front of the door. As the front bumper of the Dodge moved forward it caught the rear edge of the right fender. The damage was similar to test SS11. The Dodge was not brought to rest by the impact.	3.0	40	3.0	40	1300
SS18	41	The left corner of the Dodge front bumper struck the right door of the Honda behind the mid-length of the door, similar to tests SS12 and SS13. The door skin was dented, and the fender damage caused by test SS17 was added to. The Dodge was not brought to rest by the impact. A mark on the door ended lower than it began, owing to body roll, as in other side swipe tests. In contrast to tests SS12 and SS13, the longitudinal acceleration did not surpass 1g until the lateral acceleration did. The 3g peak likely occurred at the door leading edge where the door skin was deformed around the stiff frame of the door leading edge.	3.0	50	2.0	30	1400
SS19	42	The Honda was oriented at a larger angle to the longitudinal axis of the Dodge. Initial contact occurred between the left corner of the Dodge front bumper and the back of the Honda right door. Denting of the door skin was increased due to bumper contact as well as from contact with the Dodge fender, resulting in a scrape and dent above the trim line on the Honda door. The Dodge was brought to rest by the collision and the two vehicles remained in contact. There were lateral accelerations of larger duration and amplitude than the other tests due to the increased angle.	2.5	40	2.5	120	1400

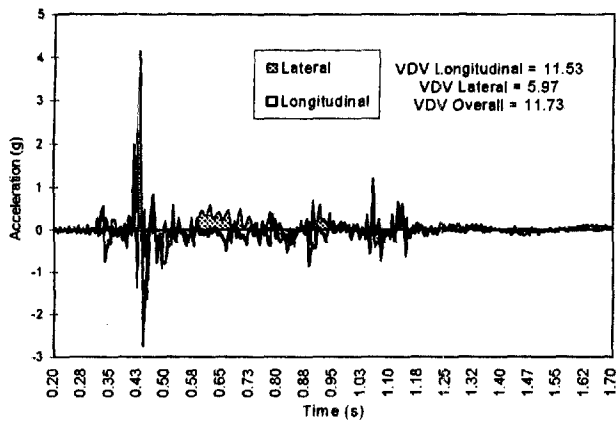


Figure 35. Acceleration for test SS8. Damage at right.

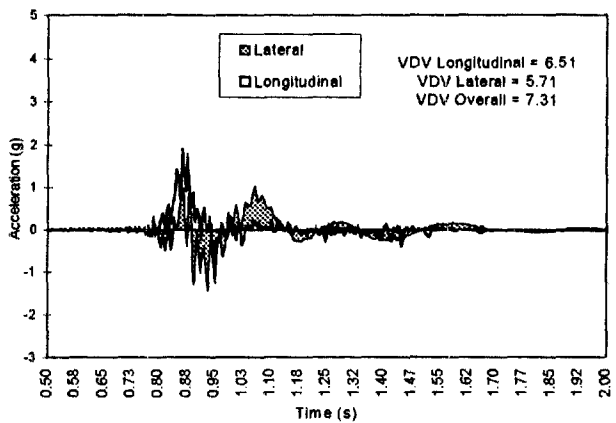
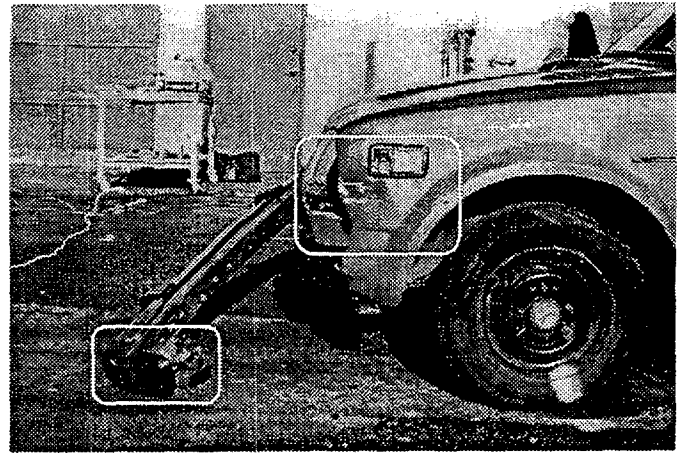


Figure 36. Acceleration for test SS10. Damage at right.

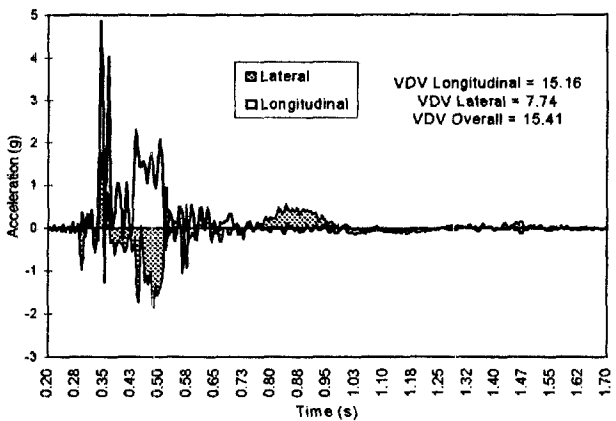
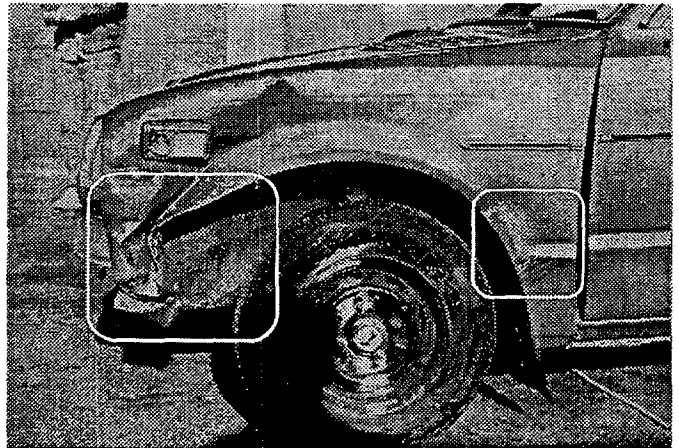


Figure 37. Acceleration for test SS11. Damage at right.

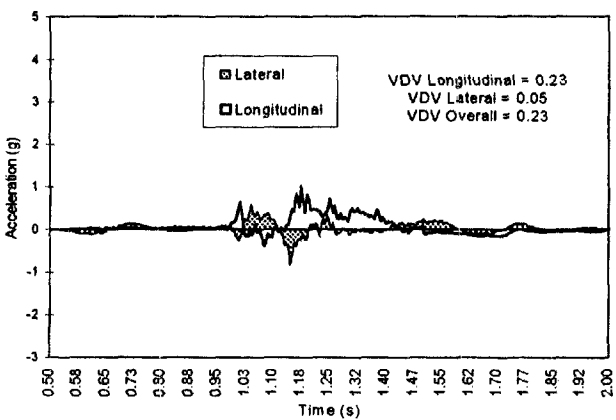
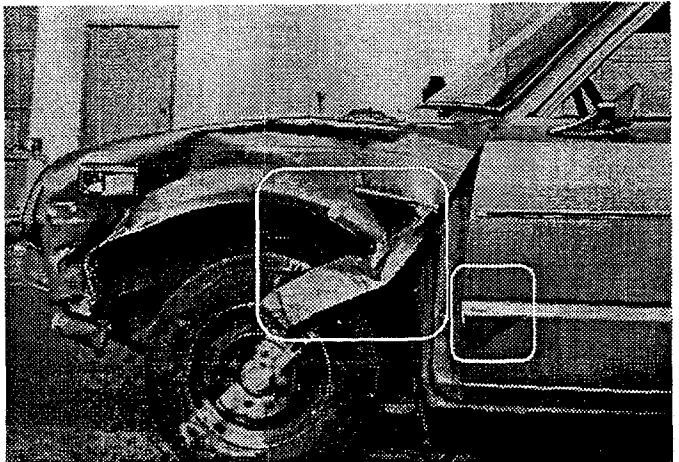
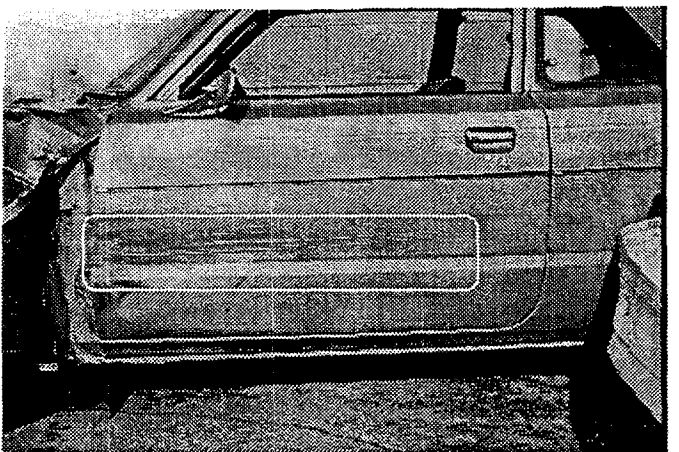


Figure 38. Acceleration for test SS12. Damage at right.



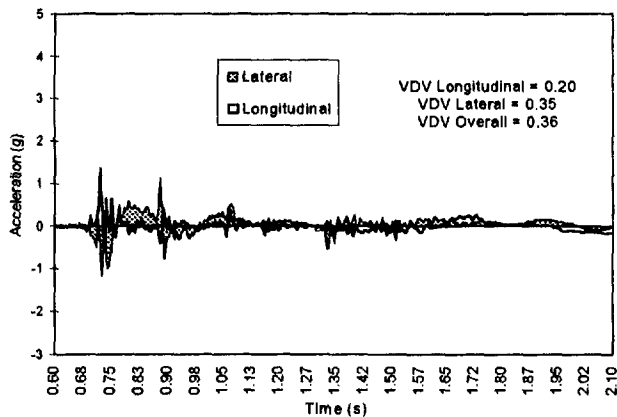


Figure 39. Acceleration for test SS13. Damage at right.

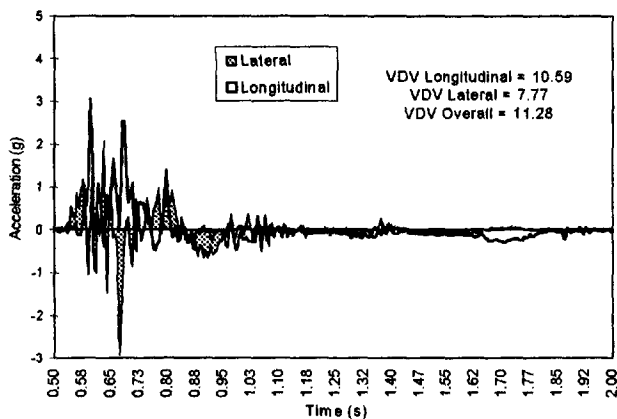
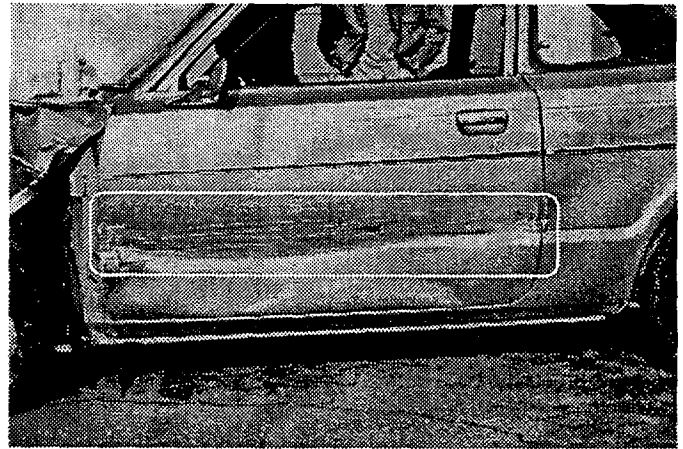


Figure 40. Acceleration for test SS17. Damage at right*.

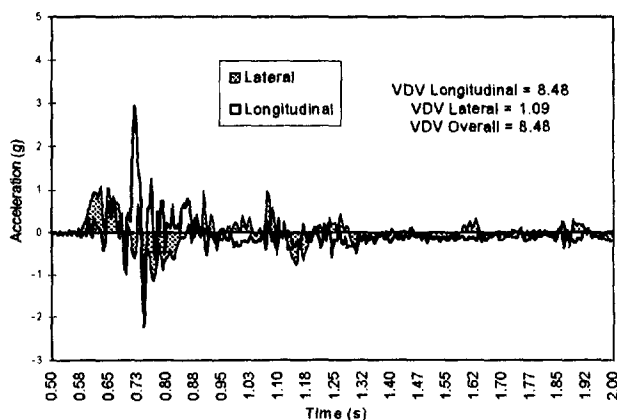
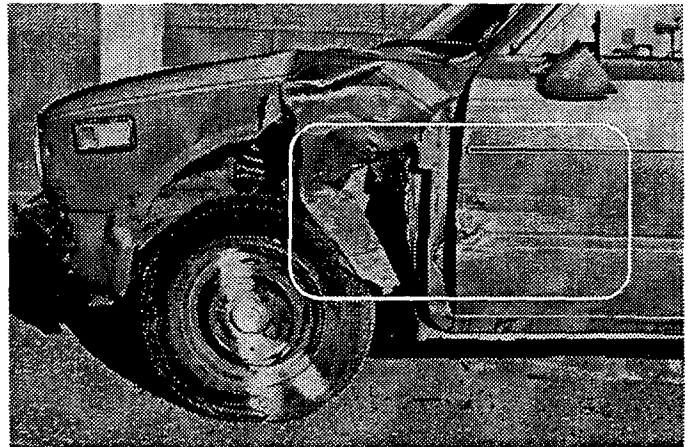


Figure 41. Acceleration for test SS18. Damage at right*.

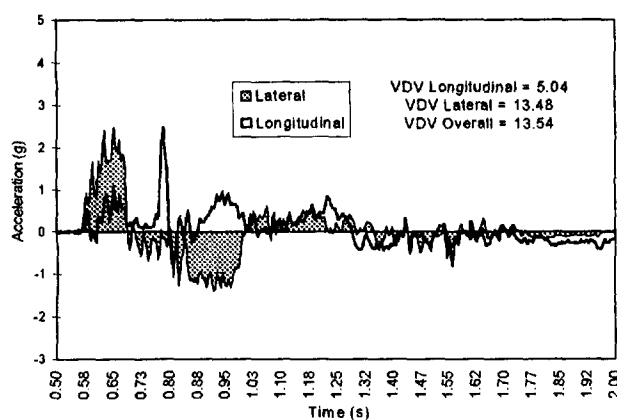
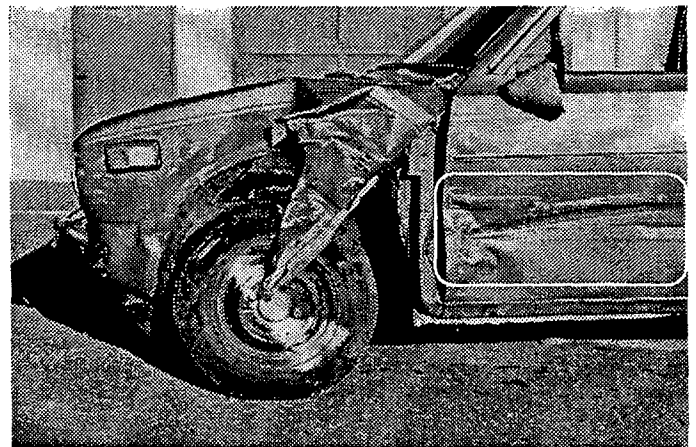
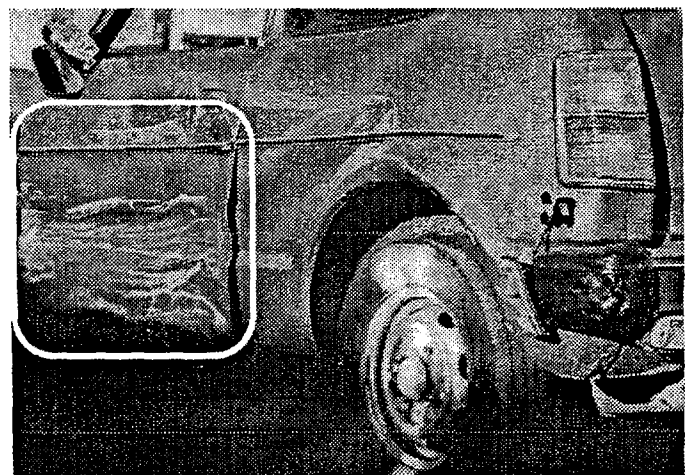


Figure 42. Acceleration for test SS19. Damage at right*.



* Damage is to *right* side. Image mirrored for comparison to previous figures.

SIDE SWIPE TEST ACCELERATIONS. In the eleven side swipe tests the motion imparted to the target vehicle consisted of a longitudinal and lateral disturbance that lasted on the order of one second. Longitudinal accelerations were characterized by short duration (less than 50 ms) impulses that were associated with snagging or other mechanical blocks to the forward progress of the bullet vehicle. These peaks rose above a background of sub-1g longitudinal oscillations. Lateral accelerations were predominantly less than 1g, except for short duration peaks that occurred when there was snagging and in the last test where the angle between vehicles was not shallow, and corresponded to the vehicle rolling on its suspension. These lateral accelerations were damped to zero in about one second.

Where there was no snagging, much of the disturbance was within what the car could experience during driving. Figure 43 shows the acceleration data from test 12, where there was a shallow door crease and no snagging, superimposed on the traction envelope²² for 0.8g (corresponding to dry pavement and an average forward acceleration capability of 0.3g).

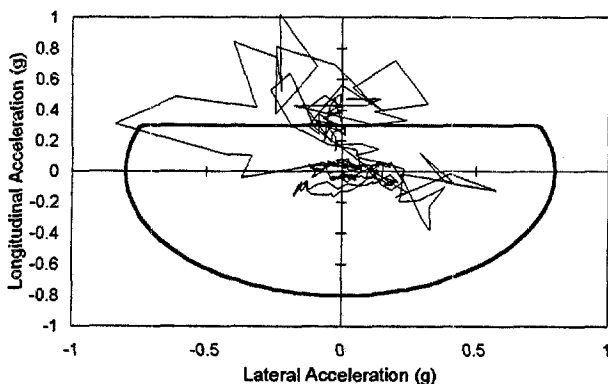


Figure 43. Accelerations in test 12 compared to driving maneuver envelope.

In order to quantify the severity of the impact for the target vehicle, the concept of *vibration dose* was used. The concept has been used to help quantify vehicle ride, seat comfort and motion sickness. It uses the acceleration-time history of a vehicle motion to compute the Vibration Dose Value (VDV) for that motion. It is applicable to vibratory motions which may be steady-state, random or transient. According to Griffin²³, the VDV can be used to characterize the motion when there are occasional peaks above the background (termed high crest factor vibrations, where crest factor is the ratio of peak to RMS acceleration). It has been suggested that a vibration dose value of $15 \text{ ms}^{-1.75}$ is a level above which some

consideration of the health effects of the vibration may be appropriate. Use of the VDV is advantageous for side-swipe collisions because it considers the effects of both peaks and background accelerations, as well as the duration of the disturbance. To attempt characterization of any impact, including a side-swipe impact, using only peak or average acceleration would ignore important information about the disturbance.

The vibration dose value is defined as follows:

$$VDV = \left[\int_{t=0}^{t=T} a^4(t) dt \right]^{1/4}$$

Griffin notes that the accelerations $a(t)$ above 80 Hz needn't be considered for motor vehicles. In the present work, accelerations above 80 Hz in the side-swipe tests were removed with spectral analysis. This had the effect of slightly lowering some of the short duration peaks. Griffin also recommends computing VDV's for each axis, in this case lateral and longitudinal. An overall VDV is defined as:

$$VDV_{\text{overall}} = \sqrt[4]{VDV_{\text{lateral}}^4 + VDV_{\text{longitudinal}}^4}$$

As a preliminary check of the applicability of the vibration dose concept, the VDV was computed for several rear-end barrier impacts for which the ΔV (the descriptor used for front and rear impacts) and acceleration history were known. The results (Figure 44) show that the VDV of $15 \text{ ms}^{-1.75}$ occurs near the 8 km/h ΔV . Recall that the 8 km/h ΔV level is near the onset of symptoms for volunteers in rear-end collisions. The slope of the VDV - ΔV curve increases as ΔV increases, so that a unit increase in ΔV at the 8 km/h level corresponds to a larger increase in VDV than at the 4 km/h ΔV level. These preliminary results are encouraging. It is noted that the VDV value is independent of direction. It appears that a VDV of 15 is near the tolerance level for rear impacts, but would be below the tolerance level for frontal impacts.

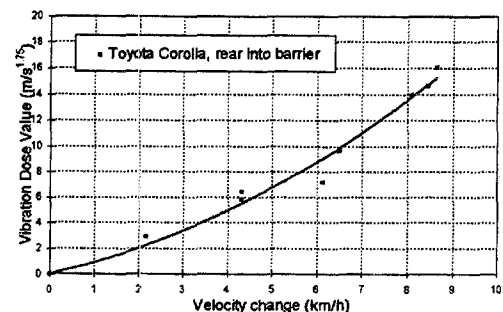


Figure 44. Comparison of VDV and ΔV for rear-end impacts.

The VDV values were computed for side-swipe tests SS8 through SS19 and 24 and tabulated in Table 14. In all cases the duration was taken as 1.5 seconds. The only test where the VDV was greater than 15 was test SS11, where the fender was snagged. If the VDV is a valid descriptor to relate vehicle motion and occupant response, then test SS11 would be roughly equivalent (i.e. have the same vibration dose and same direction of acceleration) to a rear-end impact with an 8 km/h ΔV . In tests SS12 and SS13 and 22 to 24, where there was no snagging, the overall VDV was less than 1. Tests 22 to 24 were the only side-swipes to have a volunteer in the target vehicle during the collision. The volunteer did not experience any significant displacements within the vehicle, and no discomfort was reported following those exposures, or "doses". For comparison, longitudinal and lateral VDV's of 0.317 and 0.459 were reported by Griffin for a small car on a city road. Values around 2 were reported for farm tractors.

Table 14. Target vehicle vibration dose values.

Test	Closing speed (km/h)	Lateral (m/s ^{1.75})	Long. (m/s ^{1.75})	Overall (m/s ^{1.75})
SS8	23.8	5.97	11.53	11.73
SS10	25.9	5.71	6.51	7.31
SS11	27.0	7.74	15.16	15.41
SS12	8.6	0.05	0.23	0.23
SS13	8.3	0.35	0.20	0.36
SS17	19.1	7.77	10.59	11.28
SS18	19.8	1.09	8.48	8.48
SS19	20.2	13.48	5.04	13.54
24	9.4	0.07	0.13	0.13

DISCUSSION

Several staged collision test results have been reported. The collisions are either front-end, rear-end, lateral or side-swipe. These four types of collisions constitute the bulk of minor collisions which the authors are called on to investigate. A minor collision is defined as one where tire forces and/or restitution effects are not negligible. In order to make accurate estimates of the severity of these collisions, tire force and restitution effects must be considered.

Existing vehicle crash test data can often be applied to estimate the severity of a collision. This can be done for front-end or rear-end collisions by

applying raw vehicle-to-barrier deformation data (if vehicles in a two vehicle collision have similar mass and stiffness), or from application of a momentum-energy-restitution model, or from duplicating the collision.

For lateral impacts, front or rear vehicle-to-barrier test data can be used to estimate the energy absorbed and force applied to the bullet car. Some data exist to estimate the energy absorbed by the laterally struck target vehicle from the force applied to it, or from the amount of damage. A momentum-energy-restitution model (which includes angular momentum) can be applied in the case where one axle of the target vehicle is undisplaced. If both axles are displaced, the MER model for front and rear-end collisions can be applied by accounting for tire forces at the sliding tires of the laterally struck vehicle.

The severity of side-swipe impacts has been characterized by the lateral and longitudinal acceleration history. Those accelerations can be compared to driving maneuvers (like accelerating, braking or swerving), though peak accelerations often briefly exceed those levels. Alternatively, the acceleration history can be manipulated to compute a vibration dose value, which allows comparison between side-swipe and other impacts.

Impacts where the target vehicle has a vertical or significant rotational (several degrees of yaw) component of motion have not been investigated.

Human volunteer data are available from exposures to front, rear, lateral and side-swipe impacts. The severity of these staged impacts is known precisely, and can be compared to the occupant dynamics and existence/non-existence of symptoms. From these data it can be seen that estimates of impact severity should be as accurate as possible because symptoms that have not been observed at a given level may occur at only a slightly higher level.

In the volunteer tests, it is emphasized that the occupant dynamics often lead to either no symptoms, or to symptoms that lasted for only a few days. No physiological changes lasting longer than a few days have been generated in the volunteer tests.

REAR END AND FRONT END COLLISIONS. Though front and rear impacts are dynamically similar for cars, volunteer data indicate that occupants fare better in front-end impacts than in rear-end impacts. The severity, characterized as ΔV , tends to be associated with the onset of symptoms in rear-end collisions at around 6.5 to 8 km/h ΔV and in front-end collisions at around 12 to 20 km/h ΔV .

A momentum-energy-restitution model can be used for predicting ΔV in a vehicle-to-vehicle collision from vehicle-to-barrier data. Care must be exercised when extrapolating vehicle-to-barrier data to cases with more isolator compression or damage. Estimates of energy absorption will likely be underestimated if an isolator has bottomed out.

Limited comparison of vehicle-to-barrier and vehicle-to-vehicle data suggest that some isolator equipped vehicles may have shorter impact durations in vehicle-to-barrier impacts than in vehicle-to-vehicle impacts. These differences in duration may be sufficiently large to cause strain-rate sensitive isolators to perform slightly differently in these two test types.

In a rear-end impact, many vehicles will be undamaged at severities that are above the range where human volunteers have reported neck and back symptoms. This applies to vehicles that the authors have tested, which were reported on previously and in the present work. Vehicles that do not meet the standard to which the vehicles tested were built (Canadian Motor Vehicle Safety Standard 215) may perform differently.

In a front-end impact vehicle damage may precede occupant symptoms for lap and torso belt restrained occupants, based on available volunteer data.

LATERAL COLLISIONS. The dominant motion for the target vehicle is sideways, even with both vehicles in motion.

Body panel damage can be inflicted to the target vehicle without introducing large lateral displacements. Unlike aligned impacts, the lateral impact produces a small displacement for a given ΔV . This is because the sideways motion of the car is quickly arrested by tire side forces.

Contact damage on the target vehicle is often observed to end a few cm lower on the side of the vehicle than where it began. This is due to the roll of the target, where its struck side moves upward in response to the collision force, and the downward pitch of the bullet.

The use of a momentum-energy-restitution model (including angular momentum) for predicting $\Delta\omega$ appears promising. Inputs to the model include duration (typically around 100 ms), restitution (typically 0.2 to 0.6), and pre-impact speed of the bullet vehicle. That speed can be determined from the circumstances of the collision (e.g. case of a bullet car backing out of a parking stall and hitting the side of a passing car) or by selecting it such that the predicted energy absorption matches the energy

absorption associated with the damage to the vehicles. If the bullet car has isolators, then energy absorption for that car can be predicted from vehicle-to-barrier tests. Other data must be used to predict the energy absorption of the target.

Human volunteer motion is characterized by a rocking of the upper body about the lap belt toward the struck side of the vehicle, which is actually the vehicle moving underneath the occupant. The relative displacement of the head and torso was minimal for the small number of staged collisions with a volunteer. Once the car stops moving sideways, shortly after impact, the occupant regains the seated position. Actual vehicle tests differ from sled tests; in sled tests there is more motion of the volunteer's upper body because the sled does not return to its initial velocity a short time after the onset of deceleration.

SIDE-SWIPE COLLISIONS. At low closing speeds the target and bullet vehicles are apt to stick together. At higher closing speeds the bullet vehicle will continue past the target.

As in lateral impacts, contact damage typically ends a few cm lower than where it began. This can be useful in determining the relative direction of the vehicles.

Isolator compression was observed on a bullet vehicle at an engagement angle of 16° , but not at 10° for similar impact speeds.

The target vehicle acceleration in the lateral and longitudinal directions can be characterized as a disturbance that lasts on the order of 1 second, with brief peaks (less than 50 ms) that rise above a background of sub-1g oscillations. Target vehicle lateral and longitudinal acceleration peaks were observed that exceeded values that the vehicle is capable of generating in driving maneuvers, even when there was no vehicle snagging.

Characterizing the vehicle motion in a side-swipe collision as ΔV or peak acceleration may not give a true representation of the severity of the impact. The former will have a low value because the duration is long and, except for a few peaks, the accelerations are low. The latter would only include peak values that have pulse widths typically less than 50 ms, which may be short enough not to be felt by an occupant.

Methods of integrating the acceleration history of the vehicle that are used as design guides for vehicles that are subjected to longitudinal and lateral vibrations can be applied. One method is to compute the RMS (Root Mean Square) acceleration. Or, for vibrations where the peak values are much greater than the RMS value (termed high crest factor) the vibration dose may be computed. The Vibration Dose Value

(VDV) is the fourth root of the integration of the fourth power of the acceleration-time curve. For the side-swipe collisions, the vibrations had high crest factors, so were characterized by computing the vibration dose.

In limited volunteer testing, no symptoms were reported. The VDV was below $0.13 \text{ m/s}^{1.75}$ in those tests. The VDV, computed for a rear-end collision with a ΔV of 8 km/h, was approximately $15 \text{ m/s}^{1.75}$.

HUMAN EXPOSURE. Further study of the concept of vibration dose, and similar methods applied to characterizing vehicle ride, is warranted. The vehicle motions studied in the various collision types have accelerations with directions, amplitudes and frequencies that have been studied by engineers concerned with vehicle ride and its effects on comfort and performance. Certain levels of vibration dose may be associated with reduced comfort, fatigue, or exposure limit²⁴.

There appears to be some potential to produce symptoms in human volunteers in rear-end impacts that does not appear to be present at similar severity levels in frontal and lateral impacts. Rear-end impacts are also very common. Vehicle dynamics in a rear-end impact can be viewed as a single 5 to 10 Hz cycle in the longitudinal, forward direction. Seats that are designed to minimize this type of vibration may have a positive influence on automotive safety.

ACKNOWLEDGMENT

This project would not have been possible without the efforts the entire MacInnis Engineering staff.

The authors are indebted to the following people for their assistance acquiring and instrumenting vehicles, staging collisions, and analyzing test data: David King, Gunter Siegmund, Peter Williamson Darcy Montgomery, David Garau, David Mumford and Bill Cliff.

REFERENCES

- 1 Bailey, M.N., King, D.J., Romilly, D.P., Thomson, R. "Characterization of Automotive Bumper Components for Low Speed Impacts", Proceedings of the Canadian Multidisciplinary Road Safety Conference VII, June 1991, Vancouver, BC.
- 2 King, D., Siegmund, G. and Bailey, M. "Automobile Bumper Behavior in Low-Speed Impacts", SAE #930211.
- 3 Siegmund, G.P., Bailey, M.N., and King, D.J., "Characteristics of Specific Automobile Bumpers in Low-Velocity Impacts", SAE 940916.

- 4 McConnell, W.E., et al "Analysis of Human Test Subject Kinematic Responses to Low Velocity Rear End Impacts", SAE #930889.
- 5 Campell, K. "Energy Basis for Collision Severity", SAE #740565, Society of Automotive Engineers, Warrendale, PA, 1974.
- 6 Hight, P.V. & Lent-Koop, D.B., "The Correlation Between Delta-V, Barrier Equivalent Velocity and Crush in Automobile Collisions", Proceedings of CMDRSC No. III, May 27 - 30, 1984.
- 7 Kerkhoff, J.F., Husher, SE, Varat, M.S., Busenga A.M., Hamilton, K. "An Investigation into Vehicle Frontal Impact Stiffness, BEV and Repeated Testing for Reconstruction", SAE #930899, Society of Automotive Engineers, Warrendale, PA, 1993.
- 8 ASTM E 647 - 93 Society of Automotive Engineers, Warrendale, PA, 1974. "Standard Test Method for Measurement of Fatigue Crack Growth Rates"
- 9 Howard, R.P., Bomar, J, Bare, C., "Vehicle Restitution Response in Low Velocity Collisions", SAE #931842, Society of Automotive Engineers, Warrendale, PA, 1993.
- 10 Malmsbury, R.N., Eubanks, J.J., "Damage and/or Impact Absorber (Isolator) Movements Observed in Low Speed Crash Tests Involving Ford Escorts", SAE #940912, Society of Automotive Engineers, Warrendale, PA, 1994.
11. Severy, D, Matthewson, J. and Bechtol, C. "Controlled Automobile Rear-End Collisions, An Investigation of Related Engineering and Medical Phenomena" Canadian Services Medical Journal, 1955
12. Szabo, T., Welcher, J., Anderson, R., Rice, M., Ward, J., Paulo, L., and Carpenter, N. "Human Occupant Kinematic Responses to Low-Speed Rear-End Impacts" SAE #940532 Society of Automotive Engineers, Warrendale, PA, 1994
13. Siegmund, G. and Williamson, P. "Speed Change (ΔV) of Amusement Park Bumper Cars" Canadian Multidisciplinary Motor Vehicle Safety Conference VIII, 1993
14. Chandler, R. and Christian, R. "Crash Testing of Humans in Automobile Seats" SAE #700361 SAE #940532 Society of Automotive Engineers, Warrendale, PA, 1970
- 15 Woolley, R.L., et al, "Rear Stiffness Coefficients Derived from Barrier Test Data", SAE 910120.

16. Glenn, T.
"Anthropomorphic Dummy and Human Volunteer Tests of Advanced and/or Passive Belt Restraint Systems" SAE #740579 Society of Automotive Engineers, Warrendale, PA, 1974
17. Mertz, H. and Patrick, L.
"Strength and Response of the Human Neck" SAE #710855 Society of Automotive Engineers, Warrendale, PA, 1971
18. Ewing, C. and Thomas, D.
"Human Head and Neck Response to Impact Acceleration" Naval Aerospace Medical Research Laboratory, August 1972
19. Limpert, R. and Andrews, D.
"Linear and Rotational Momentum for Computing Impact Speeds in Two-Car Collisions (LARM)" SAE #910123 Society of Automotive Engineers, Warrendale, PA, 1991
20. Willke, D. and Monk, M.
"Side Interior Stiffness Measurement" NHTSA Final Report for SRL-66, 1984
21. Zaborowski, A.
"Human Tolerance to Lateral Impact With Lap Belt Only" SAE #640843 Society of Automotive Engineers, Warrendale, PA, 1964
22. Van Valkenburgh, P.
"What's It Really Like Out There?" Road and Track October 1983
23. Griffin, M.J.,
"Evaluation of Vibration with Respect to Human Response", SAE #860047, Society of Automotive Engineers, Warrendale, PA, 1986.
24. "Guide for the Evaluation of Human Exposure to Whole Body Vibration" International Standards Organization standard ISO 2631-1978 (E)